Journal of Materials Chemistry B

ROYAL SOCIETY OF CHEMISTRY

REVIEW

View Article Online
View Journal | View Issue

Cite this: *J. Mater. Chem. B*, 2026, **14**, 1167

Recent advances in non-vascular stents for occlusive luminal disease treatment

Mian Chen, Jianfeng Yan and Yonghui Ding *

Stent placement has become a standard intervention for occlusive luminal diseases across both vascular and non-vascular systems. Beyond their well-established use in endovascular therapy, stents play essential roles in managing obstructions in non-vascular conduits such as the airway, esophagus, urethra, ocular outflow tract, bile duct, and colon. However, conventional permanent stents are frequently associated with complications such as migration, restenosis, infection, and granulation tissue formation, which often necessitate secondary removal procedures. To overcome these limitations, biodegradable stents have emerged as a promising alternative, providing temporary mechanical support before safely degrading *in situ*. In parallel, drug-eluting stents offer site-specific therapeutic delivery to modulate local tissue responses, suppress fibrosis, and reduce infection risk. Although coronary stent technologies are extensively reviewed, an integrated analysis of biodegradable and drug-eluting stent innovations for non-vascular applications remains lacking. This review addresses this gap by systematically evaluating current and emerging stent technologies for major non-vascular luminal diseases. We examine the interplay between material properties, device mechanics, and the unique pathophysiological challenges of each anatomical site. We further highlight recent advances in biodegradable and drug-eluting stent design, discuss key barriers to clinical translation, and provide a forward-looking perspective on future directions in non-vascular stent development.

Received 25th June 2025,
Accepted 6th December 2025

DOI: 10.1039/d5tb01514f

rsc.li/materials-b

Department of Biomedical Engineering, Worcester Polytechnic Institute, Worcester, MA 01609, USA. E-mail: yding7@wpi.edu

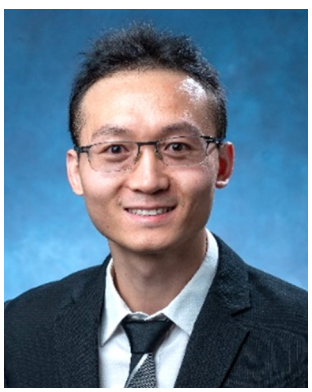

Yonghui Ding

Dr Yonghui Ding is an Assistant Professor in the Department of Biomedical Engineering at Worcester Polytechnic Institute, where he leads a research group focused on the design and additive manufacturing of biomaterials for tissue regeneration. He is committed to the education and training of the next generation of the regenerative engineering workforce. Dr Ding earned his PhD in Mechanical Engineering from Hong Kong University of Science and Technology, completed postdoctoral training in Mechanical Engineering at the University of Colorado Boulder, and previously served as a Research Assistant Professor in Biomedical Engineering at Northwestern University.

1. Introduction

Occlusive luminal diseases encompass a broad spectrum of conditions affecting tubular structures throughout the body, categorized into vascular and non-vascular luminal diseases (NVLDs). While occlusive vascular diseases primarily involve the occlusion or stenosis of arteries, such as coronary arteries, NVLDs affect luminal organs across multiple organ systems. These include the digestive system (esophagus, gastrointestinal tract, biliary ducts), respiratory system (airways), urinary system (ureters, urethra), and specialized structures such as ocular drainage pathways.[1] The pathogenesis of NVLDs frequently involves inflammation and subsequent scar tissue formation, either as complications of surgical interventions or manifestations of inflammation-associated diseases. Malignant processes also contribute significantly to luminal obstruction, particularly in gastrointestinal and respiratory systems. Without appropriate intervention, NVLDs can result in severe morbidity, including respiratory distress, dysphagia, hematuria, and potentially life-threatening complications.

Treatment strategies for luminal obstruction span a spectrum from conservative medical management to invasive surgical intervention. Available options include surgical resection, laser ablation, balloon dilation, pharmacologic therapy, and stent placement. Among these approaches, stenting has

emerged as the preferred minimally invasive intervention due to its ability to rapidly restore luminal patency while minimizing tissue trauma. Stents, typically constructed from metals or polymers, are deployed to mechanically support the lumen, reopening obstructions and reducing the risk of restenosis. The evolution of stent technology, from early rigid plastic tubes to flexible three-dimensional (3D) mesh structures, has significantly improved stent performance and ease of deployment. However, conventional stents constructed from permanent, non-degradable materials remain associated with significant complications. These include device migration, restenosis from tissue hyperplasia, biofilm formation leading to infection, and the necessity for subsequent removal procedures.

To move beyond mitigating complications and instead actively combat these biological failure modes, drug-eluting stents (DESs) have been developed. This technology, which revolutionized interventional cardiology, involves coating a stent with a polymer carrier that releases a therapeutic agent in a controlled manner. In coronary arteries, DESs eluting anti-proliferative drugs effectively prevent restenosis by inhibiting the smooth muscle cell proliferation that narrows the vessel after intervention. Inspired by this success, DES technology is now being adapted to address the unique challenges of non-vascular applications. Rather than just providing passive mechanical support, non-vascular DESs are designed to actively modulate the local environment by eluting a variety of agents, such as anti-proliferative drugs to prevent granulation tissue formation, chemotherapeutics to treat local malignancies, or antimicrobial agents to combat infection. This represents a paradigm shift from a purely mechanical solution to a combined mechano-biological therapeutic platform.

Addressing the challenge of permanent implants, biodegradable stents (BDSs) represent another transformative technology. These devices provide temporary structural support to diseased lumens while undergoing controlled degradation, ideally leaving behind repaired and functional tissue.[2] By eliminating removal procedures, BDSs offer substantial clinical advantages including reduced patient morbidity and healthcare costs. Nevertheless, clinical translation faces significant obstacles. Current biodegradable materials often exhibit insufficient mechanical strength for certain applications, unpredictable degradation kinetics that vary with local pH and enzymatic activity, and inflammatory responses triggered by degradation byproducts such as lactic acid from poly(L-lactic acid) (PLLA).

While extensive literature exists reviewing coronary stent technology,[3–6] a comprehensive analysis of non-vascular stent applications remains limited. This article addresses this critical gap by providing detailed coverage of stent technologies for common NVLDs, including airway stenosis, esophageal stricture, ureteral obstruction, glaucoma, biliary stricture, and colonic obstruction (Fig. 1). For each application, we systematically examine disease pathophysiology, commercially available stents currently in clinical use (Table 1), and associated complications. Crucially, we integrate recent advances in both biodegradable and drug-eluting technologies within each section, highlighting how these innovations aim to overcome the specific biological and mechanical challenges of each organ system. This review serves as a comprehensive resource for

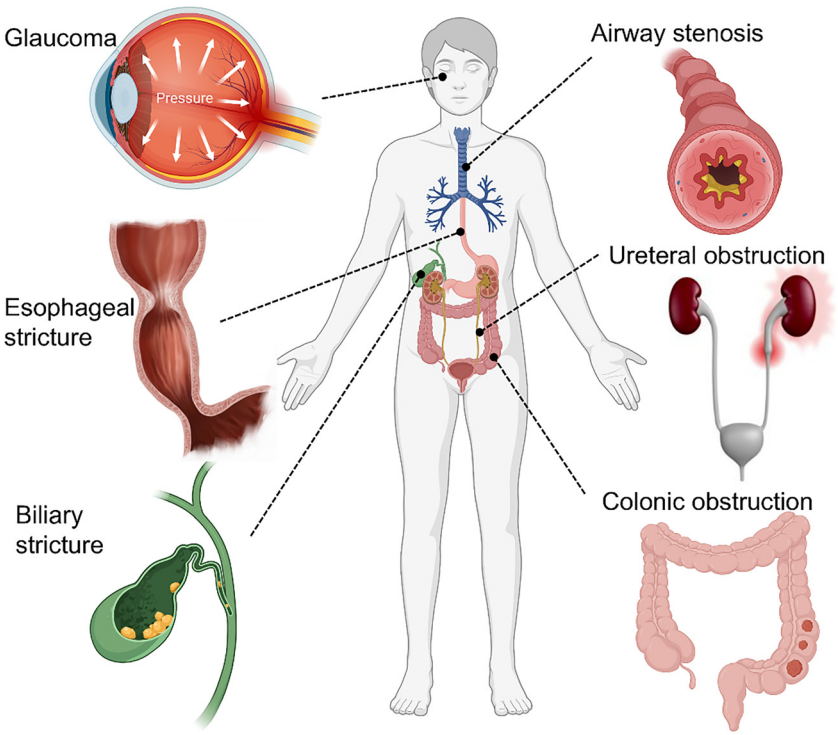

Fig. 1 Common occlusive non-vascular luminal diseases that are often treated by stent placement (figure was created with https://Biorender.com).

Table 1 Summary of commercially available stents for the treatment of various NVLDs

Diseases	Stent name	Producer	Materials	Permanent or biodegradable	Advantages	Common issues
Airway stenosis	Ultraflex™ Tracheobronchial stent	Boston scientific	Nitinol with silicone covering	Permanent	• Flexible bronchoscopy delivery • Minimal stent migration • Strong mechanical properties	• High perforation and bleeding risks • Difficult relocation and removal • High granulation tissue ingrowth
	AERO™	Alveolus	Nitinol with polyurethane coating	Permanent		
	Dumon stent	Novatech	Silicone	Permanent	• Low granulation tissue ingrowth • Customized shape and mechanical properties • Easy relocation and removal	• High stent migration rates • Rigid bronchoscopy delivery • High secretion blockage
	DV stent tracheal	Ella-CS	Polydioxanone	Biodegradable	• Low risks of stent migration • Mild granulation tissue ingrowth • Customized shape and design	• Rigid bronchoscopy delivery • Low mechanical properties • High cost
Esophageal stricture	Ultraflex™ Esophageal NG stent	Boston scientific	Nitinol with silicone covering	Permanent	• Low stent migration • Strong mechanical properties	• High granulation tissue ingrowth • Difficult removal • High rigidity (causing chest pain, tissue damage, bleeding, *etc.*)
	Wallflex™ Esophageal stent	Boston scientific	Nitinol with silicone covering	Permanent		
	Polyflex™	Boston scientific	Polyurethane with silicone covering	Permanent	• Low cost • Easy delivery and removal • Mild granulation tissue ingrowth	• High migration rates
	SX-ELLA	Ella-CS	Polydioxanone	Biodegradable	• Mild granulation tissue ingrowth • Customized shape and parameters • Low stent migration	• Low mechanical properties • High cost • High stricture recurrence
Ureteral obstruction	Imajin Hydro™	Coloplast	Silicone	Permanent	• High flexibility • Low encrustation rate • Low infection rate	• Low passage efficacy • Hard delivery • Low tensile strength
	Percuflex™ Plus	Boston scientific	Polyurethane	Permanent	• High tensile strength • High passage efficacy	• High stiffness (causing discomfort and pain) • High encrustation rate • High infection rate
Glaucoma	iStent™/iStent™ Inject	Glaukos corporation	Titanium	Permanent	• Safe profile • Effective IOP reduction	• Hard implantation • High medication utilization
	Hydrus™ Microstent	Ivantis, alcon	Nitinol	Permanent	• Safe profile • Effective IOP reduction	• Hard implantation • Medium medication utilization
	XEN™ Gel stent	Allergan	Porcine collagen/glutaraldehyde	Permanent	• Low medication utilization • Effective IOP reduction • Safe profile	• High needling rate • High bleb fibrosis/scar formation
Biliary stricture	WallFlex™ Biliary PLUS RX stent	Boston scientific	Nitinol with silicone covering	Permanent	• Low stent migration • Strong mechanical properties • High stent patency	• High tissue overgrowth • Difficult relocation and removal
	HANAROSTENT®	OLYMPUS	Nitinol	Permanent	• Low stent migration • Strong mechanical properties • High stent patency	• High tissue overgrowth • Difficult relocation and removal • Unavailable for benign stricture
	Advanix™	Boston scientific	Polypropylene	Permanent	• Easy delivery and removal • Low cost	• High bile sludge • High stent migration

Table 1 (*continued*)

Diseases	Stent name	Producer	Materials	Permanent or biodegradable	Advantages	Common issues
Colonic obstruction	Wallflex™ Colonic stent	Boston scientific	Nitinol	Permanent	• Minimal stent migration • Flexible gastroscope delivery • High mechanical properties • High stent patency	• High tumor ingrowth • High perforation rates

clinicians, researchers, and medical device developers working to advance NVLDs treatment through innovative stent-based approaches.

2. Development of stent materials and fabrication technologies

2.1. Fundamental design requirements

Permanent stents provide durable mechanical support and remain indispensable for malignant or severe non-vascular luminal obstructions. However, their long-term indwelling nature predisposes them to migration, infection, hyperplasia, and the need for complex removal. BDSs were developed to overcome these limitations by offering temporary mechanical scaffolding that gradually disappears as the tissue remodels, making them especially valuable for benign strictures and pediatric applications. Biodegradable, drug-eluting stents further advance this concept by actively interacting with luminal tissues during the critical healing period (Fig. 2). While maintaining luminal patency, these stents provide controlled release of therapeutic agents that modulate tissue responses, such as inhibiting fibroblast proliferation, reducing inflammatory signaling, and promoting re-epithelialization depending on the anatomical site. As the scaffold resorbs, chronic mechanical irritation is minimized, and locally delivered therapeutics can support functional tissue healing or regeneration. Here, we summarize the key design criteria required to ensure the efficacy and safety of stents across diverse non-vascular luminal environments.

(1) Adequate mechanical properties: stents must provide sufficient radial force to maintain luminal patency against external compression while exhibiting adequate flexibility to conform to natural luminal anatomy. The balance between radial strength and flexibility varies significantly across applications. Airway stents require resistance to dynamic compression during coughing, while esophageal stents must withstand peristaltic forces without causing erosion.

(2) Biocompatibility: materials must minimize adverse biological responses including inflammation, thrombosis, and

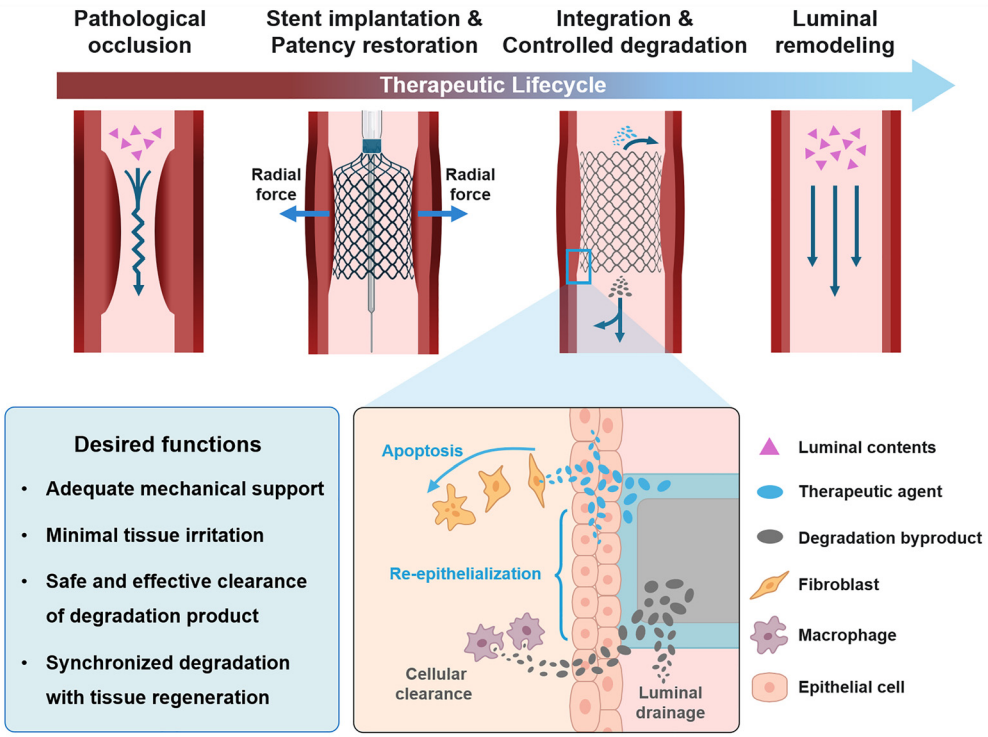

Fig. 2 Schematic illustration of the desired tissue-stent interaction for an ideal biodegradable, drug-eluting stent.

immune reactions. Surface chemistry plays a crucial role in determining protein adsorption, cellular adhesion, and subsequent tissue responses. Modern stents often incorporate surface modifications to enhance biocompatibility.

(3) Ease of delivery: design features must facilitate minimally invasive delivery through narrow lumens with smooth navigation and controlled deployment at target sites. Self-expanding designs have largely replaced balloon-expandable systems in non-vascular applications due to superior conformability.

(4) Imaging visibility: radiopacity enables precise positioning during delivery and facilitates post-procedural monitoring. Many polymer stents incorporate radiopaque markers to overcome inherent radiolucency.

(5) Complication mitigation: engineering approaches must address application-specific complications. Covered stents reduce tissue ingrowth but increase migration risk. Surface texturing and anti-migration features such as external studs or flanged ends help anchor the device while drug-eluting coatings actively modulate tissue responses.

(6) Synchronized degradation with tissue regeneration: BDSs must provide temporary mechanical support that persists throughout the critical healing window and then degrade in synchrony with tissue remodeling. Precise control of degradation kinetics is essential. Premature degradation can lead to early stent collapse and re-obstruction, whereas excessively slow degradation increases the risk of chronic foreign body reactions, inflammation, and impaired healing.

2.2. Stent materials from metals to polymers

The choice of materials for stents used in NVLDs depends on the specific clinical application and patient requirements. The materials commonly employed can be categorized into two major groups: metals and polymers. Either of these materials can be permanent or bioresorbable.

Permanent stents for NVLDs are primarily fabricated from either metallic materials or medical-grade silicone. Commonly used metals include stainless steel, cobalt–chromium alloys, and nickel–titanium alloys (nitinol) owing to their excellent mechanical strength, corrosion resistance, and biocompatibility. However, the inherent rigidity of many metallic materials, combined with the mesh-like geometry of stents, can lead to adverse events such as lumen wall injury, perforation, and excessive tissue hyperplasia, often resulting in restenosis. To address these limitations, nickel–titanium alloys have emerged as a preferred material due to their superelasticity and shape-memory properties, which enable better conformity to dynamic luminal environments and reduce the risk of mechanical trauma.[7,8] To further improve biocompatibility and reduce tissue ingrowth, many metallic NVLDs stents are partially or fully coated with polymeric membranes, such as expanded polytetrafluoroethylene (ePTFE), which provide a physical barrier while maintaining structural support.[9–11] Alternatively, silicone-based stents are widely used for their high compliance, flexibility, and minimal tissue reactivity. However, despite these advantages, silicone stents are prone to migration, particularly in high-mobility luminal environments, and are associated with complications such as secretion accumulation, infections, and lumen obstruction.[12]

BDSs are fabricated from either biodegradable polymers or biodegradable metallic materials, each exhibiting distinct degradation mechanisms and limitations (Table 2). Polymeric BDSs degrade primarily through hydrolysis of ester bonds, in which water molecules cleave the polymer backbone into oligomers and monomers that can be metabolized or cleared from the body.[13] Commonly used biodegradable polymers include polylactic acid (PLA), poly(glycolic acid) (PGA), polydioxanone (PDO), poly(L-lactic acid) (PLLA), poly(lactic-*co*-glycolic acid) (PLGA), and polycaprolactone (PCL). These materials exhibit variable degradation times: PLLA and PCL typically degrade slowly over one or more years,[14,15] whereas PLGA and

Table 2 Comparative summary of key properties of commonly used biodegradable polymers (PLA, PDO, PLGA) and Mg-based alloys

Feature	Biodegradable polymers (PLA, PDO, PLGA)	Magnesium-based alloys
Mechanical strength	• PLA: highest strength, brittle • PLGA: moderate strength • PDO: flexible, good tensile strength	• Excellent radial strength
Degradation mechanism	• Hydrolysis	• Electrochemical erosion
Degradation rate	• PLA: slowly over one or multiple years • PLGA/PDO: about 10 weeks	• 1–2 weeks
Degradation in acidic environment	• Minimal effect for pH = 3.0–7.0 • Accelerated for pH < 3.0	• Very rapid • Uncontrolled
Degradation in alkaline environment	• Accelerated	• No effect
Inflammatory response	• Local pH decreases from acidic byproducts (lactic acid and glycolic acid) • Acidosis-driven inflammation • Risk of fibrosis	• Mg^{2+}: generally anti-inflammatory • H_2: potential antioxidant • OH^-: mild alkalization may counteract inflammation

PDO degrade within approximately 10 weeks.[16] Notably, local luminal environments strongly modulate hydrolytic kinetics. Both alkaline and strongly acidic conditions accelerate ester hydrolysis relative to neutral pH.[17] Mildly alkaline conditions, such as the biliary tract (pH 7.8–8.6), significantly enhance base-catalyzed hydrolysis of polyester chains.[18] In contrast, the native esophagus (pH 6.0–7.0) and colonic (pH 5.5–6.5) environments are only weakly acidic and do not markedly accelerate degradation. However, gastroesophageal reflux can transiently reduce esophageal pH to 2–4, substantially accelerating acid-catalyzed ester cleavage.[18] Highly hydrated lumens such as the airway, biliary tract, and urinary lumens promote rapid water penetration into the polymer, further accelerating hydrolytic degradation. Polymer degradation behavior can be tuned by modifying molecular weight, crystallinity, cross-link density, and porosity. However, polymeric stents generally possess lower radial strength than metals, limiting their use in high-load luminal environments. Additionally, their acidic degradation products (*e.g.*, lactic and glycolic acids) are known to locally decrease pH and trigger chronic inflammation.

To overcome these limitations in biodegradable polymers, biodegradable metallic stents, particularly those made from magnesium (Mg)-based alloys, have gained increasing attention. Mg is inherently biocompatible and naturally present in the human body. In physiological environments, Mg undergoes electrochemical corrosion, producing magnesium hydroxide and hydrogen gas; the transient local alkalinization and hydrogen release can influence tissue healing. However, magnesium hydroxide is unstable in chloride-rich body fluids, resulting in rapid, uncontrolled degradation and early loss of mechanical integrity.[19] To regulate degradation, a variety of surface modification and bulk alloying strategies have been developed. Biodegradable polymer coatings, such as poly(3-hydroxybutyrate-*co*-3-hydroxyhexanoate) (PHBHHx) or poly(1,3-trimethylene carbonate) (PTMC), act as temporary diffusion barriers that dampen early corrosion.[20,21] More advanced approaches, including ion implantation, modify the surface chemistry and microstructure without altering device geometry. Implanting elements, such as zirconium (Zr) or titanium (Ti), into Mg alloys can generate dense, protective layers composed of implanted species and their oxides, effectively shielding the underlying Mg from corrosive environments and substantially reducing corrosion rates.[22,23] Beyond surface treatments, bulk material engineering offers another avenue for improvement. For example, Mg–Zn composites reinforced with *in situ*-formed nanoparticles create a refined, multiphase microstructure that enhances mechanical strength through synergistic strengthening while reducing degradation by promoting electrochemical homogeneity.[24] Collectively, these advances are enabling the development of Mg-based stents with more predictable and tunable degradation profiles, improved mechanical durability, and clinically relevant functional lifetimes.

2.3. Stent fabrication technologies

Stents are commonly fabricated using two conventional methods: selective laser cutting and braiding. Selective laser cutting is widely adopted due to its high precision, efficiency, and ability to produce intricate and complex geometries. Typically, polymeric or metallic materials are first extruded into tubular forms. A laser is then used to cut away excess material, yielding the desired three-dimensional (3D) stent architecture.[25] However, this process can introduce surface defects, such as microcracks and machining stripes, and induce residual stresses that compromise mechanical performance.[26] To address these issues, post-processing techniques like electropolishing are employed to smooth edges and remove surface imperfections. Alternatively, weaving involves interlacing metal or polymer fibers into controlled patterns, such as braiding or knitting, to form tubular structures.[27,28] Braided stents offer excellent axial flexibility and tunable radial strength, depending on the braiding configuration. However, compared to laser cutting, weaving has limited capability for producing complex geometries.

Additive manufacturing, or 3D printing, has emerged as a transformative approach in stent fabrication, enabling the production of patient-specific devices tailored to an individual's anatomy, including customized size, geometry, and mechanical behavior. Common 3D printing techniques used in stent fabrication include selective laser melting (SLM), fused deposition modeling (FDM), and digital light processing (DLP). SLM employs a high-power laser to selectively melt and solidify fine metal or polymer powders layer by layer. Materials such as stainless steel, cobalt–chromium (CoCr), and bioresorbable polymers like PGA and PLGA have been processed *via* SLM to produce stents.[28,29] However, SLM-printed stents typically exhibit high surface roughness ($R_a > 10$ μm) due to partially sintered particles, leading to dimensional inaccuracies that necessitate post-polishing for surface refinement.[30] FDM is a cost-effective 3D printing method that extrudes heated thermoplastic filaments onto a rotating mandrel. Common materials include polycaprolactone (PCL) and poly(L-lactic acid) (PLLA).[31–33] However, low resolution of FDM often results in thick struts (>200–300 μm), which may be undesirable for vascular applications. A modified FDM setup using a solvent-based PLLA ink and a 200 μm nozzle achieved a reduced strut thickness of 80 μm *via* controlled solvent evaporation.[34] Nevertheless, overlapping extruded filaments remain a challenge for producing low-profile stents with this method. DLP, a high-resolution and high-speed technique based on light-induced polymerization of photocurable inks, offers a solution for thin-strut stent fabrication. In 2016, personalized bioresorbable stents with 150 μm strut thickness were fabricated using a microscale continuous liquid interface production (μCLIP) process and a photocurable citrate-based polymer.[35] Recent advancements by our group have further improved this technique, enabling the batch fabrication of eight stents with 10 mm in length and a minimum strut thickness of 65 μm in just seven minutes, achieving a throughput of one stent per minute.[36,37]

2.4. Translational barriers for 3D-printed stents

Despite these advancements, the clinical translation of 3D-printed stents faces major challenges spanning materials,

manufacturing, and regulatory quality assurance. A key limitation is the restricted palette of printable biomaterials. Many clinically established materials, such as medical-grade silicone, are incompatible with high-resolution additive manufacturing, while high-precision technologies such as digital light processing (DLP) are constrained to a narrow range of proprietary photocurable resins. One workaround has been the use of 3D-printed molds for silicone casting, enabling the fabrication of anatomically tailored silicone stents.[38] Beyond material constraints, technical challenges in the printing process itself can compromise device performance. For example, overhanging geometries often require sacrificial support, and their removal may damage surface quality or weaken structural features.[39] However, the most significant barrier remains the establishment of robust pathways for standardization and quality control. The clinical adoption of patient-specific devices depends on reliable, non-destructive methods to verify internal architecture, detect printing defects, and ensure mechanical reliability, highlighted by the need to transition micro-CT imaging from a research tool to a routine quality-control modality.[40] Ultimately, achieving batch-to-batch consistency is essential, as it underpins the predictable performance required for regulatory approval and safe clinical use.

3. Airway stent

3.1. Airway stenosis and treatments

Airway stenosis, characterized by the narrowing of the trachea or bronchus, can result in symptoms such as chronic coughing, respiratory distress, and in severe cases, death due to asphyxiation (Fig. 3a). This pathological narrowing frequently arises from excessive scar tissue formation and is a common complication of tuberculosis, prolonged intubation, and lung transplantation. For example, post-tuberculosis tracheobronchial stenosis is observed in approximately 10–40% of patients during the healing phases due to fibrotic tissue remodeling and necrosis.[41] Similarly, post-intubation tracheal stenosis may develop in 6–21% of cases, often triggered by prolonged cuff pressure and mucosal injury.[42] Additionally, up to 27% of lung transplant recipients experience airway stenosis, primarily due to ischemia and immune rejection at the anastomotic site.[43]

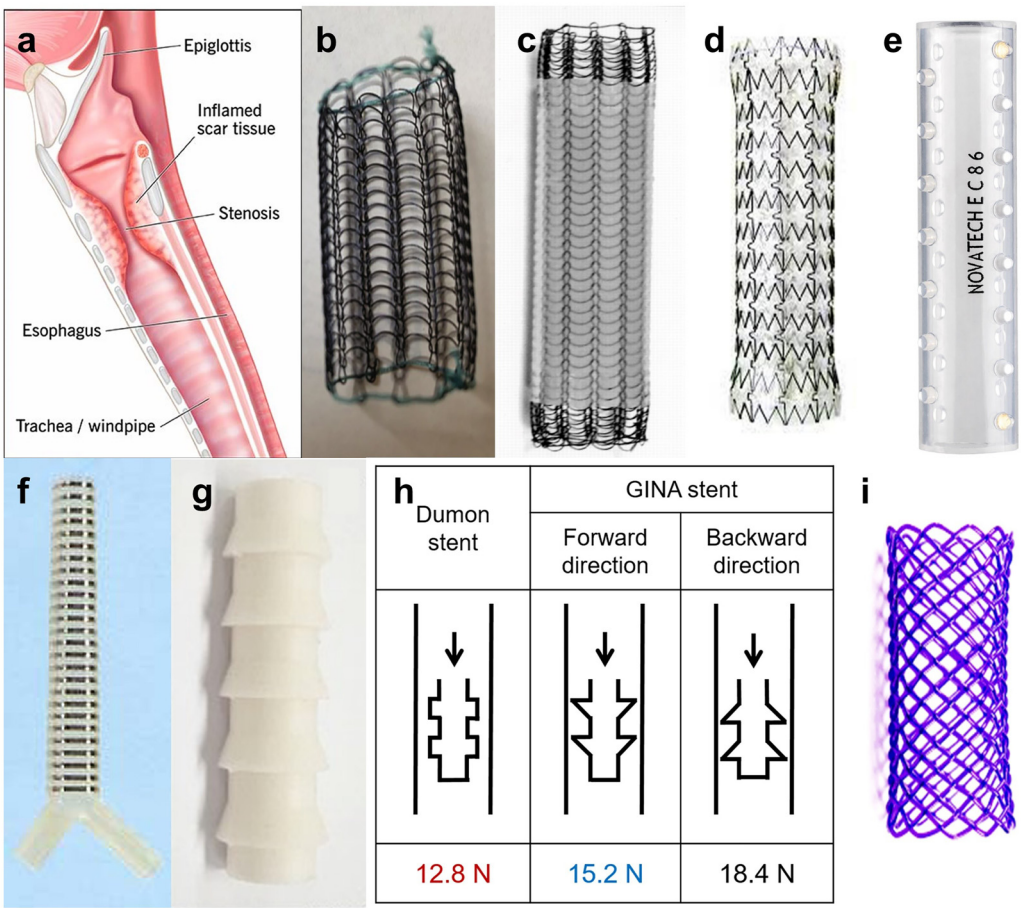

Fig. 3 (a) Airway stenosis. (b) Uncovered metallic stent (Ultraflex™, Boston Scientific). (c) Fully covered metallic stent (AERO™, Alveolus). (d) Partially covered metallic stent (Ultraflex™, Boston Scientific). (e) Dumon stent (Novatech). (f) Dynamic™ (Y) stent (Boston Scientific). (g) GINA stent; (h) anti-migration force of the GINA stent and Dumon stent. (i) Biodegradable DV stent tracheal (ELLA stent, Ella-CS).

Surgical resection, involving the excision of the stenotic airway segment followed by end-to-end anastomosis, is considered the gold standard for managing airway stenosis, with a reported success rate exceeding 91%.[44] However, this approach is suitable for only about 10% of patients due to significant limitations, such as comorbidities, the length of the stenotic segment, prior tracheal surgeries, and risks associated with general anesthesia.[45] Consequently, less invasive endoscopic interventions are often preferred for the majority of patients. These include balloon dilation and laser ablation, which offer temporary symptom relief but are often insufficient for long-term airway patency. In contrast, stent placement has emerged as the most widely used palliative treatment for maintaining airway patency over extended periods. Stents serve as internal scaffolds that mechanically support the airway and provide immediate relief from breathing difficulties.

3.2. Stents in the treatment of airway stenosis

3.2.1. Overview: biomechanical environments and complications. Airway stents are subjected to cyclic changes in transmural pressure from respiration and large transient pressure spikes from coughing. To accommodate this biomechanical environment, the ideal airway stent must provide adequate radial force to resist tracheal collapse and be sufficiently flexible to follow airway curvature and motion.[46] Insufficient radial force to counter airway recoil or cough-induced shear will lead to stent migration. An overly rigid stent can generate high stress concentrations at the stent-tissue interface, leading to mucosal injury, granulation tissue overgrowth, and even the formation of aerodigestive fistulas.[47,48] Furthermore, the physical presence of enclosed stents can mechanically inhibit mucociliary clearance by compressing the cilia, leading to mucus plugging and recurrent infections.[49] Therefore, the ideal design must balance mechanical support with the preservation of physiological function.

Airway stents are typically delivered *via* bronchoscopy using a guidewire, with outer diameters ranging from 8–20 mm and lengths between 15–70 mm. Two major categories dominate current clinical practice (Table 1): metallic stents (*e.g.*, Ultraflex™, Aero™, and Bona) and silicone stents (*e.g.*, Dumon, Dynamic™). Despite their widespread use, both types are associated with complications that vary according to their material properties and structural design. For instance, rigid metallic stents with strong radial force are often associated with high risks of granulation tissue overgrowth, while excessively flexible stents are prone to migration.[50] Fully covered stents with impermeable membranes, while limiting tissue ingrowth, also block mucus drainage, leading to mucus retention and increased risk of infection.[51]

3.2.2. Metallic airway stents. Metallic airway stents are generally classified into self-expandable and balloon-expandable types and are fabricated from materials such as stainless steel or nitinol. These stents are further categorized as uncovered, partially covered, or fully covered based on their surface coatings (Fig. 3b–d). Uncovered stents, composed entirely of metal mesh, demonstrate low migration rates (2.2–6.4%)[52] and reduced mucus accumulation,[53] but they are prone to excessive granulation tissue formation, with rates as high as 57%.[54] To mitigate this issue, fully covered stents incorporate a silicone or polymer membrane that isolates the metal mesh from surrounding tissues. While this design reduces granulation tissue rates to 20–35%, it introduces new challenges, including higher migration (18–22%) and secretion blockage (12.5–23%).[54,55] Partially covered stents aim to balance these risks by maintaining uncovered mesh at the ends to anchor the device more securely.

However, metallic stents also pose serious risks such as perforation and bleeding, often triggered by repetitive airway movement due to coughing or breathing. As a result of these complications, the U.S. Food and Drug Administration (FDA) has issued caution against the routine use of metallic stents for benign airway disease.[56] In response, newer metallic stents fabricated from nitinol offer improved flexibility and shape memory, reducing trauma and improving compliance with dynamic airway conditions.[57,58] Despite their advantages, nitinol stents are typically regarded as permanent implants, and removal becomes problematic once granulation tissue infiltrates the mesh structure.

3.2.3. Silicone airway stents. Silicone stents, such as the Dumon stent introduced in the 1980s, are considered the gold standard for managing benign airway stenosis. These stents often feature external studs that reduce the risk of migration (Fig. 3e). Clinical studies have reported symptomatic relief in over 90% of patients shortly after stent placement.[59] Compared to metallic stents, silicone stents are associated with lower granulation tissue formation, typically around 15.7%, and the granulation that does occur is generally localized at the ends of the stent, making removal easier and less invasive.[60]

Given the strong adaptability of silicone materials, the shape and mechanical properties of silicone stents can be tailored to patient-specific needs. Nonetheless, migration and mucus retention remain major complications, with reported rates of approximately 25% and 23.8%, respectively.[60] When complications arise, silicone stents are easier to reposition or remove than metallic stents. Advanced designs such as the Dynamic™ (Y) stent incorporate horseshoe-shaped stainless steel reinforcements embedded in the anterior and lateral surfaces to mimic the biomechanical behavior of airway cartilage (Fig. 3f).[57,58] This design improves anchorage and dynamic flexibility, though placement typically requires a laryngoscope, complicating the insertion process. More recently, the GINA stent has been introduced as a novel silicone device incorporating triangular studs to enhance anti-migration performance (Fig. 3g and h). Preclinical studies in porcine models suggest the GINA stent exhibits superior resistance to migration compared to the Dumon stent.[61] However, further validation in studies with a larger number of animals and clinical trials is needed due to limitations in sample size and follow-up duration.

3.2.4. Biodegradable airway stents. Given the limitations of both metallic and silicone stents, including migration, granulation tissue formation, and high infection rates, biodegradable

stents have emerged as a promising alternative for temporary airway support. These stents are designed to gradually degrade after fulfilling their mechanical functions, thereby eliminating the need for surgical removal and reducing long-term complications. For instance, the DV stent tracheal (Fig. 3i) made of polydioxanone (PDO) was evaluated in a rabbit model, showing only a mild inflammatory response that resolved as the stent degraded.[62] More recently, advanced digital light processing (DLP)-based 3D printing has enabled the fabrication of patient-specific biodegradable airway stents using dual-polymer inks composed of poly(D,L-lactide-*co*-ε-caprolactone) (PDLLA-*co*-PCL) (Fig. 4a). These stents closely mimic the elastomeric behavior of commercial silicone stents while offering the advantages of biodegradability and anatomical customization.[63] Mechanical testing revealed that the biodegradable stents provide superior radial load-bearing capacity compared to silicone stents, particularly under large deformations (Fig. 4b). *In vitro* cytocompatibility assays with human lung epithelial cells (A549) showed no significant cytotoxicity, and accelerated degradation tests confirmed substantial mass loss (40%) after 6 weeks at 50 °C (Fig. 4c). Under physiological conditions (37 °C), the stents began degrading at the 12th week and lost 20% of their mass by 20 weeks. *In vivo* studies in rabbits indicated no stent migration and visibility for at least 7 weeks. While acute inflammation was observed at the 2-week mark, histology revealed normal tissue morphology without signs of inflammation by 10 weeks. While biodegradability successfully eliminates the problem of a permanent implant, these stents do not actively address the acute biological responses of granulation tissue formation or infection during their indwelling period, paving the way for the next generation of functionalized stents.

3.2.5. Drug-eluting airway stents. The evolution from passive mechanical support to active biological modulation represents a fundamental advance in airway stent technology. DESs deliver therapeutic agents directly to stenotic sites, maximizing local efficacy while minimizing systemic toxicity. Unlike vascular applications where preventing smooth muscle proliferation is paramount, airway DES must address dual challenges: inhibiting granulation tissue formation from hyperactive fibroblast proliferation and preventing bacterial colonization in the mucus-rich respiratory environment.[64]

For inhibiting granulation tissue, various anti-proliferative and anti-inflammatory agents have been investigated. Sirolimus (rapamycin), an mTOR inhibitor widely successful in coronary DES, has shown promising results in airway applications. A biodegradable PLLA–PCL stent loaded with sirolimus demonstrated sustained drug release, effectively reduced scar and normal fibroblast proliferation *in vitro*, and significantly decreased fibrosis with only a mild inflammatory response *in vivo*.[65] Paclitaxel is another widely studied anti-proliferative drug. A paclitaxel-eluting stent was shown to significantly reduce granulation tissue compared to bare metal stents in animal models, though clinical translation has been challenging, as the drug can inhibit the healing of mucosal epithelial cells alongside fibroblasts.[64,66] Other agents like mitomycin C, a potent fibroblast inhibitor, have also shown promise. In a 12-week animal study, a mitomycin C-eluting stent reduced tracheal stenosis by half compared to standard silicone stents, highlighting the potential of local chemotherapy to maintain airway patency.[67]

To combat infection, a major cause of morbidity and stent failure, antibacterial agents have been incorporated into stent coatings. A shape memory polymer stent with a porous structure was loaded with ciprofloxacin, demonstrating significant antibacterial activity against common airway pathogens.[68] Similarly, a silicone stent coated with allicin, a compound derived from garlic, showed favorable mucosal healing and a significant reduction in attached bacteria in a rabbit model.[69] These approaches aim to prevent the formation of bacterial biofilms, which are notoriously difficult to treat with systemic antibiotics and are a primary driver of chronic inflammation and granulation tissue.[51,64]

Despite the promising preclinical results, the clinical translation of airway DESs faces significant hurdles. A key challenge is optimizing the drug release kinetics to provide a therapeutic effect over several weeks to months without causing local toxicity.[64] The cytotoxic properties of anti-proliferative drugs, for example, could impair normal epithelial healing

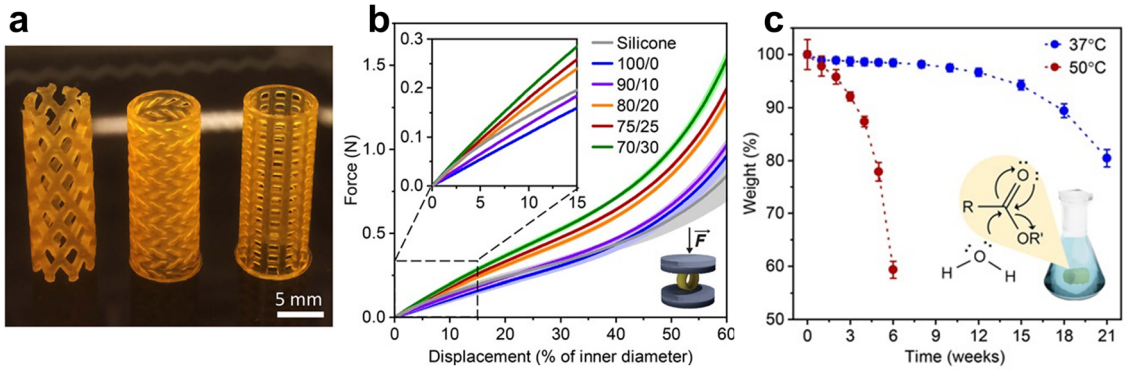

Fig. 4 (a) 3D-printed biodegradable stents with different designs. (b) Force–displacement curves of dual-polymer stents with different ratio and a NOVATECH silicone stent. (c). Degradation characterized by changes in polymer stent weight over time at physiological (37 °C) and accelerated (50 °C) conditions.

and increase the risk of complications like fistula formation.[70] Furthermore, the complex, dynamic environment of the airway, with constant mucus flow and mechanical stress from breathing and coughing, makes it difficult to design a durable drug carrier that ensures predictable release. While many animal studies show success, the lack of large-scale, long-term clinical trials means that the true efficacy and safety of airway DES in human patients remain to be established.

4. Esophageal stents

4.1. Esophageal stricture and treatments

Esophageal stricture refers to a pathological narrowing of the esophageal lumen, typically stemming from inflammation, fibrosis, or tumor growth (Fig. 5a). While the healthy esophageal diameter measures approximately 30 mm, strictures can reduce this to 13 mm or less, causing dysphagia as the primary symptom. The incidence of esophageal stricture in the U.S. is estimated at approximately 95 per 100 000 person-years, with an overall rate of about 11 per 100 000 person-years worldwide.[74] Strictures may be benign, with peptic strictures, resulting from gastroesophageal reflux disease (GERD), accounting for nearly 80% of benign cases.[75] Other benign causes include caustic ingestion, particularly in children. Malignant strictures are mostly caused by esophageal cancer. Benign strictures are often effectively managed by endoscopic dilation, with success in over 90% of patients. Mechanical (bougie) dilators are preferred for simple strictures larger than 10 mm, while balloon dilators are utilized for more complex cases.[76] Adjunctive therapies, such as intralesional steroid injections or systemic steroids, may be administered to mitigate post-dilation inflammation and reduce recurrence. In contrast, malignant strictures are primarily treated with surgical resection, chemotherapy, or radiotherapy.

4.2. Stents in the treatment of esophageal stricture

4.2.1. Overview: biomechanical environments and complications. Esophageal stents experience repetitive high-amplitude peristaltic contractions and substantial longitudinal motion of the esophageal wall due to the axial shortening during swallowing and respiration, making stent migration a primary failure mode. Peristaltic waves can overcome stent anchoring, driving stent migration. Although rigid stents resist esophageal motion, they often provoke chest pain or spasm when their axial flexibility is insufficient. Therefore, the core biomechanical conflict lies in optimizing the stent's radial force. It must be high enough to anchor the device and prevent migration, yet low enough to avoid complications like chest pain, bleeding, or perforation.[77,78] Indeed, studies show that low-radial-force stents can reduce severe adverse events without compromising efficacy.[79,80] Beyond radial force, geometric factors like wall thickness and flaring are critical, as a

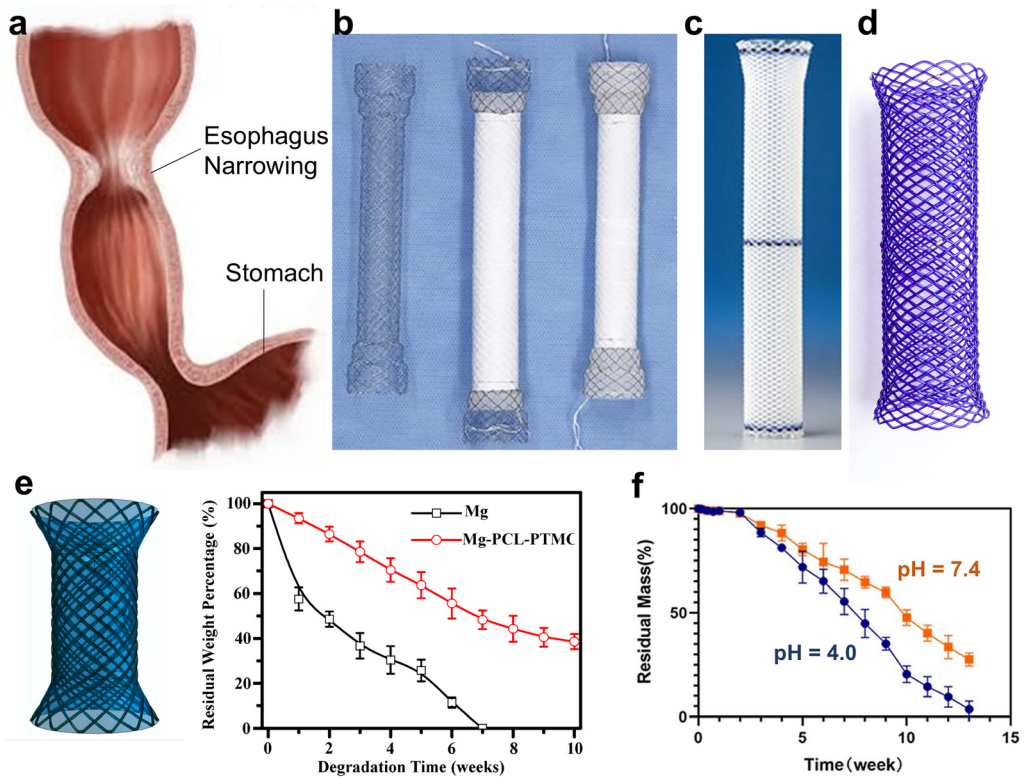

Fig. 5 (a) Schematic to show esophageal stricture. (b) Uncovered, partially covered, and fully covered SEMS (EGIS, S & G Biotech). Image was adapted from ref. 71. (c) Plastic stent (Polyflex™, Boston Scientific). (d) Biodegradable stent (SX-ELLA, Ella-CS). (e) The design of PCL–PTMC-coated Mg-based degradable stents and their degradation rate in PBS (pH 7.4). Images were adapted from ref. 72. (f) Degradation rates of PLGA-coated Mg-based degradable stents in PBS with pH 4.0 and pH 7.4. Image was adapted from ref. 73.

mismatch with the patient's anatomy can lead to food bolus impaction and reflux symptoms.[81,82]

Esophageal stenting is a cornerstone palliative therapy for patients with advanced esophageal malignancy, as more than 50% of those with late-stage disease require stents to restore luminal patency for oral intake.[83] Stents are also frequently used in refractory benign strictures, although their efficacy remains limited, with clinical success rates typically around 40–50%.[84] Esophageal stents are implanted endoscopically in a compacted state and deploy to self-expand against the lumen, improving dysphagia. Ideal esophageal stents, typically 16–21 mm in diameter and 90–150 mm in length, with a flared proximal end of 20–25 mm,[85] must resist migration, minimize tissue ingrowth, be biocompatible, and maintain sufficient radial strength. Current commercially available options include self-expanding metallic stents (*e.g.*, Ultraflex™) and self-expanding plastic stents (*e.g.*, Polyflex™), both of which are subject to complications such as migration, tissue ingrowth, or granulation tissue formation. In the past two decades, the biodegradable stents have been developed to overcome some limitations and complications of stent removal associated with self-expanding metallic stents and plastic stents.

4.2.2. Metallic esophageal stents. Self-expanding metallic stents (SEMS) fabricated from nitinol or stainless steel are the most commonly used esophageal stents for malignant strictures,[86] which are available as uncovered, partially covered, or fully covered variants (Fig. 5b). Uncovered SEMS, introduced in the 1990s, are prone to tumor ingrowth in 17–36% of cases and cause chest pain in 12–14% of patients.[87] Fully covered SEMS significantly reduce tumor ingrowth (to ~16%) and chest pain (to ~10%),[39] but migration rates increase to 23–31%.[88] Partially covered SEMS, which leave mesh exposed at the ends, help prevent migration, reducing its incidence to approximately 15%, while also lowering tumor ingrowth to around 11%.[39] However, expanding the stent diameter and size of the stent ends increases the risk of pressure-related complications, such as hemorrhage, perforation, fistula formation, fever, and pain.[89] Innovative designs such as double-layered nitinol stents with an uncovered outer layer for anchorage and a covered inner layer to suppress tumor growth have shown promising early results, with migration rates of ~4.7% and tumor embedding at ~11%.[90]

4.2.3. Plastic esophageal stents. Self-expanding plastic stents (SEPS), exemplified by the Polyflex™ stent made of thermoplastic polyurethane (PU) and silicone-covered mesh (Fig. 5c), were developed to reduce the tissue damage and chest pain associated with rigid metal stents. Compared to SEMS, SEPS typically show mild tissue damage, leading to low tissue ingrowth rates (~3.4%).[85] However, their migration, ranging from 47–67%, remains significantly higher than SEMS.[91,92] Comparative trials with SEPS *versus* SEMS in malignant strictures have reported higher late migration rates for SEPS.[91] Nonetheless, because Polyflex™ is the only FDA-approved self-expanding stent for benign strictures, its removability and safety profile make it particularly suitable in that setting.[93]

4.2.4. Biodegradable esophageal stents. To overcome the challenge of stent removal and reduce long-term complications like tumor ingrowth, granulation, and migration, biodegradable stents have been introduced. Two primary types are used clinically for benign esophageal strictures: the poly-L-lactic acid (PLLA) stent (Marui Textile Machinery) and the SX-ELLA stent (ELLA-CS; Fig. 5d). PLLA stents, consisting of knitted PLLA monofilaments,[94] were implanted into 13 patients with various esophageal diseases. The result showed no re-narrowing during the following 7 months to 2 years, while 10 patients experienced stent migration.[95] SX-ELLA stents, which are made of woven polydioxanone (PDO) monofilament and CE-approved in Europe,[96] has been evaluated in a meta-analysis involving 16 studies and 246 patients.[97] Technical success was excellent (97.2%) with clinical success (symptom resolution) in 41.9% of cases. Re-intervention was required in 36.2%, while migration occurred in only 6.5%, and reported complications occurred in 15% of patients. Early PLLA stents suffered from rapid degradation and loss of radial force, leading to collapse and restenosis. In contrast, the SX-ELLA stent maintained structural integrity for at least 6–8 weeks after placement and degraded by 90% within 9–12 weeks, offering more sustained dilation.[98] In 2011, Rincon *et al.* reported a patient receiving an SX-ELLA stent showing a collapse of the stent mesh inside the esophageal lumen, which might be due to the partial absorption of PDO mesh and reduced mechanical strength.[99]

Biodegradable metal stents, particularly Mg-based alloys, are under development due to their mechanical strength and biocompatibility. However, a significant challenge associated with Mg-based materials is their rapid degradation rate, resulting in 50% mass loss *in vitro* within 1 week.[100] To address this challenge, Yuan *et al.* used mixed polymer of PCL and PTMC as the coating on Mg alloy stents, which significantly slowed down the degradation from 100% mass loss at 7 weeks for pristine Mg stent to 40% mass loss at 10 weeks for coated stent (Fig. 5e).[72] The coated stent also showed good elasticity and safety after placement in rabbits for 4 weeks. In another study, Liu *et al.* introduced a PLGA polymer coating containing paclitaxel as an antiproliferative drug on a Mg alloy stent.[73] The addition of PLGA coating increased radial force of stent by 2.5 times and achieved controlled degradation over 13 weeks (Fig. 5f). The evaluation of stents in rabbit models showed that stents maintained esophageal patency for at least 3 weeks with reduced infiltration of inflammatory cells and fibrous tissue. However, the stent migration rate of 58.3% (7 out of 12 rabbits) remains high. While these advancements in biodegradable materials are promising, they primarily address the issue of permanence and mechanical support. The fundamental challenges of preventing tissue ingrowth in benign strictures and inhibiting tumor progression in malignant cases remain, setting the stage for the development of drug-eluting stents.

4.2.5. Drug-eluting esophageal stents. To actively modulate the biological responses that lead to stent failure, DESs have been developed to provide localized, sustained pharmacotherapy directly at the site of the esophageal stricture. Reflecting the dual nature of esophageal strictures, the therapeutic goals of

DES in this application are fundamentally different from those in the airway. For malignant strictures, the primary objective is local tumor control through the elution of chemotherapeutic or radioactive agents. In stark contrast, for benign strictures, the goal shifts to preventing hyperplastic tissue response and restenosis, often using anti-proliferative or anti-inflammatory drugs.[100] This targeted approach aims to overcome the limitations of both permanent stents and systemic drug administration by maximizing local drug concentration while minimizing off-target toxicity.[101]

For malignant strictures, the primary goal of DES is local tumor control. Stents have been designed to elute chemotherapeutic agents to inhibit tumor growth and prolong stent patency. For instance, a biodegradable magnesium stent coated with paclitaxel (PTX) in a poly(lactic-*co*-glycolic acid) (PLGA) carrier was shown to enhance fibroblast apoptosis and reduce inflammatory cell infiltration in a rabbit model.[73] Another innovative approach involves a magnetic field-responsive stent coated with a PTX-loaded film containing a phase-change material. This design allows for on-demand drug release triggered by an external alternating magnetic field, offering a new level of control over local chemotherapy.[102] In addition to chemotherapy, radioactive stents loaded with iodine-125 seeds have been developed for palliative brachytherapy. A meta-analysis of studies on esophageal cancer showed that radioactive stents resulted in better dysphagia relief and longer overall survival compared to traditional SEMS.[103]

In the context of benign strictures, DES are designed to elute anti-proliferative or anti-inflammatory drugs to prevent the hyperplastic tissue response that causes restenosis. A novel polymer-free DES was developed by creating a nanonetworked silica film on the surface of a nitinol stent.[104] This film served as a reservoir for sirolimus, an anti-proliferative agent, and was shown to significantly inhibit stent-induced tissue proliferation in a rat model. Another strategy employed a biodegradable electrospun paclitaxel/poly(ε-caprolactone) (PCL) fiber coating on a bare stent.[105] In a dog model, this DES markedly reduced inflammation and collagen hyperplasia and was easily extracted with minimal tissue damage, demonstrating the potential of combining biodegradability with drug elution to manage benign strictures.

Despite significant preclinical success, the clinical translation of esophageal DES has been slow and met with considerable challenges. A primary hurdle is achieving optimal drug release kinetics; an initial burst release can cause local toxicity, while an overly slow release may be sub-therapeutic.[106,107] The complex esophageal environment, with constant peristalsis and fluid flow, makes predictable, long-term drug delivery difficult.[107] Furthermore, *in vitro* models often fail to accurately predict *in vivo* drug uptake, which is highly dependent on the permeability of the esophageal tissue.[108] While numerous animal studies have demonstrated proof-of-concept, there is a notable lack of large-scale human clinical trials for esophageal DES. Consequently, their definitive role in improving patient outcomes, particularly in terms of overall survival and long-term patency for malignant disease, remains to be established.[107]

5. Ureteral stents

5.1. Ureteral obstruction and treatments

Ureteral obstruction is a blockage in one or both ureters, which are the tubes that carry urine from the kidney to the bladder (Fig. 6a). If left untreated, this condition can result in hydronephrosis, recurrent urinary tract infections, kidney damage, or even renal failure. Obstruction impedes the normal flow of urine, causing it to back up into the kidneys and increasing the risk of infection and pressure-induced damage. Common symptoms include flank pain, hematuria (blood in the urine), and difficulty urinating. The most common causes of ureteral obstruction include benign prostatic hyperplasia (BPH), kidney stones, and ureteral stricture due to scar tissue formation. BPH, or prostate gland enlargement, affects approximately 70% of men over the age of 60 and is driven by age-related hormonal changes that promote prostate cell proliferation.[109] The enlarged prostate can compress the prostatic urethra and obstruct urine flow. Kidney stones, solid crystalline aggregates composed primarily of calcium oxalate, calcium phosphate, or uric acid, can physically block the ureter. According to the National Health and Nutrition Examination Survey (NHANES), the prevalence of kidney stones in the U.S. population was 10.1% in 2015–2016,[110] and the incidence is increasing globally. Ureteral strictures may also result from post-surgical complications, particularly following procedures for kidney stone removal. Iatrogenic injury during ureteroscopic intervention can lead to inflammation and subsequent scar tissue formation. A prior study reported a 14.3% incidence of ureteral obstruction in patients undergoing kidney stone removal surgery.[111] Treatment of ureteral obstruction depends on the underlying cause. For BPH, medical therapy with FDA-approved drugs such as finasteride is commonly used. Finasteride inhibits 5-alpha-reductase, reducing dihydrotestosterone levels and leading to prostate shrinkage, thereby relieving urethral compression. For kidney stones, a ureteroscope is advanced through the urinary tract to directly visualize the stones, which are then fragmented using laser lithotripsy and extracted with a retrieval basket.

5.2. Stents in the treatment of ureteral obstruction

5.2.1. Overview: biomechanical environments and complications. The ureter is a narrow, highly curved conduit that undergoes coordinated, unidirectional peristaltic contractions propagating from the renal pelvis to the bladder. These contractions generate repetitive radial compression and axial propulsion forces on implanted stents, which can contribute to stent migration. Continuous low-amplitude peristalsis also produces persistent friction between the stent surface and the urothelium. This micro-trauma disrupts the protective mucosal barrier and serves as a major initiator of biofilm formation and mineral encrustation.[112–115] In addition, the complex flow

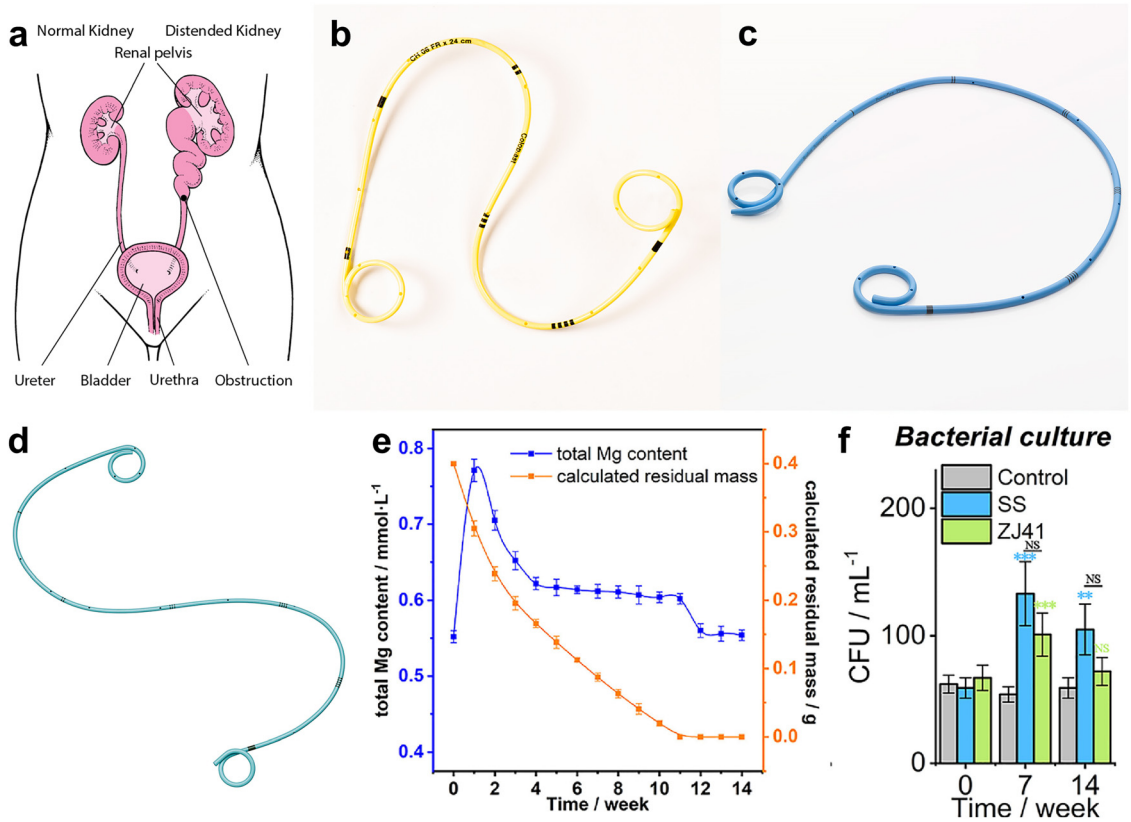

Fig. 6 (a) Ureteral obstruction. (b) Silicone stent (Imajin Hydro™, Coloplast). (c) PU stent (Percuflex™ Plus, Boston Scientific). (d) The Tria™ stent (Boston Scientific) (e) the changes of total urine magnesium content and the calculated residual mass of the ZJ41 Mg stents as a function of time. (f) Bacteria concentration results of the control group (no implantation), stainless steel stent (SS), and ZJ41 stent at 0-, 7- and 14 weeks post-implantation.

patterns generated around stent features, particularly side holes, create regions of low wall shear stress (WSS), which are well-established sites for bacterial adhesion and crystal deposition.[116] As a result, a central challenge in ureteral stent design is achieving high material lubricity and an optimized geometry that minimizes friction- and flow-induced biological complications.

Ureteral stents are commonly placed following kidney stone removal procedures to maintain ureteral patency and prevent postoperative complications. Stents are typically inserted using a flexible cystoscope and guidewire to ensure reliable urine drainage and to minimize risks of early or delayed ureteral obstruction.[117] Standard ureteral stents typically have a diameter of 1.5–5 mm and a length of 12–30 cm.[118] The most commonly used design is the double-J stent, named for its curled ends that anchor in the renal pelvis and bladder, preventing migration. Side holes are often incorporated to promote urine flow even when the ureter is partially compressed. Currently available ureteral stents are composed primarily of silicone (*e.g.*, Pyelostent, Imajin Hydro™, Endosil™), PU (*e.g.*, Percuflex™, Polaris™ Ultra, Tecoflex™), and metallic stents (*e.g.* Resonance®, Passage™). Global usage of ureteral stents exceeds 1.5 million annually, with market projections estimating values surpassing $564.4 million by 2026.[119] Despite their widespread use, ureteral stents are associated with a high incidence of complications, including bacterial infections and encrustation, which affect over 80% of patients. The urinary system presents a challenging environment to implanted stents due to fluctuating pH, the continuous presence of various microorganisms and mineral salts in urine. These conditions contribute to early complications, occurring in 10–50% of patients within the first week of stent placement, and nearly universal complication rates with long-term stenting beyond four weeks.[120] Upon exposure to urine, stents become coated with a urinary conditioning film, composed of urinary proteins, ions, and crystals. This film promotes bacterial adhesion and colonization, which has been reported in 42–90% of indwelling stents.[121] Bacterial colonization not only increases infection risk but also accelerates encrustation, a late-stage complication involving mineral deposition on the stent surface that can obstruct urine flow and necessitate surgical removal. These complications, particularly infection, encrustation, and stent obstruction, can lead to stent failure, significantly reducing patient quality of life and imposing a substantial economic burden on healthcare systems.

5.2.2. Silicone stents. Silicone was one of the earliest materials used for ureteral stents due to its softness and flexibility compared to other materials. It has long been recognized for its resistance to encrustation and bacterial adhesion, which are key advantages demonstrated in both *in vivo* and

in vitro studies. For example, a prospective randomized multicenter trial of silicone Imajin Hydro™ (Coloplast) (Fig. 6b) *versus* PU-based Percuflex Plus™ (Boston Scientific) (Fig. 6c) in 141 post-ureteroscopy patients found significantly lower biofilm formation (0.93 *vs.* 1.24, $p = 0.0021$) and mineral encrustation (0.78 *vs.* 1.22, $p = 0.0048$) in the silicone group after just three weeks.[122] Long-term *in vitro* studies have similarly confirmed that smooth silicone surfaces resist struvite and hydroxyapatite buildup more effectively than PU and other polymers.[123,124] However, earlier silicone stents were abandoned due to practical limitations: high friction during placement, low tensile strength, and narrow lumen-to-wall thickness ratios that impeded urine flow and made guidewire insertion difficult. Recent advancements in silicone chemistry and stent design have addressed these issues. Modern silicone exhibits improved tensile strength and hydrophilic coatings, which significantly reduce friction during placement and enhance patient comfort. A pivotal clinical comparison between the modern Imajin Hydro™ and Percuflex Plus™ stents showed that silicone stents were associated with significantly lower pain scores at day 20 post-implantation (body pain index: 18.7 *vs.* 25.1, $p = 0.015$), indicating better patient tolerance.[125] These findings underscore the therapeutic potential of modern silicone ureteral stents, combining the anti-encrustation benefits of traditional silicone with enhanced delivery and durability properties.

5.2.3. Polyurethane stents. PU became the material of choice for ureteral stents after early silicone models were discontinued, primarily due to its enhanced tensile strength, mechanical resilience, and reliable urine drainage performance. However, PU's rigidity often results in increased patient discomfort and stent-related pain.[126] Furthermore, PU stents exhibit significant encrustation rates, ranging from 27% after 6 weeks, 57% between 6–12 weeks, and reaching 76% beyond 12 weeks, as well as bacterial colonization in approximately 55% of devices.[127] To mitigate these drawbacks, manufacturers have developed PU-based copolymers and surface coatings, such as hydrogels, hydrophilic layers, and antimicrobial agents, to reduce encrustation and biofilm formation. Products like Percuflex™, Polaris Ultra™, and Tecoflex™ claim improved durability and decreased complication rates. Nonetheless, detailed composition data are largely proprietary, and independent comparative studies remain scarce. A notable innovation is Boston Scientific's Tria™ stent, featuring a PercuShield™ technology, which is a nonionic, super-smooth, hydrophobic inner and outer surface coating (Fig. 6d). Initial *in vitro* and short-term *ex vivo* studies showed that the Tria™ stents with PercuShield coatings resulted in up to 60% reduction in calcium and Mg salt deposition compared to other PU stents.[128] However, a randomized clinical trial comparing Tria™ to the Polaris Ultra™ stent over 14 days found no significant difference in encrustation volume, as measured by micro-computed tomography.[129] While these early results support the feasibility of Tria™, its long-term *in vivo* effectiveness and patient outcomes remain to be demonstrated in extended studies.

5.2.4. Metallic stents. Metallic ureteral stents have been developed to address the mechanical limitations of traditional silicone and PU stents, which can deform or collapse under external compression from tumors, fibrotic tissue, or crossing anatomical structures such as blood vessels.[113] These compressive forces are especially common in malignant obstructions, where polymer-based stents often fail to maintain ureteral patency. In contrast, metal stents offer superior radial strength and mechanical durability, making them suitable for more severe or recurrent cases of ureteral obstruction. Among these, double-J stents like the Resonance®, constructed from nickel–cobalt–chromium–molybdenum alloy, are designed to resist external forces while reducing migration. Self-expandable metal stents, such as the Memokath® 051, utilize shape-memory alloys that expand *in situ* to conform to the ureteral lumen, providing reliable long-term drainage. Clinical studies have demonstrated that these metallic stents are effective in managing both benign and malignant obstructions, often achieving months of patency, though complications such as stent migration, encrustation, hematuria, and urinary tract infections are still observed.[130] To improve the patient's comfort, newer generations of metal stents, such as the Passage™, have been engineered for greater flexibility and anatomical conformity.[131] These designs also maintain strong resistance to radial compression, a key requirement for treating extrinsic obstruction. Early data suggested improved performance in select patient populations,[131] but broader clinical validation is still needed. Long-term safety, optimal sizing, and prevention of complications like biofilm formation remain critical areas for future research to fully establish the role of next-generation metal stents in urological practice.

5.2.5. Biodegradable stents. Traditional ureteral stents often require a second procedure for removal once their therapeutic function is no longer needed, a process that adds to patient discomfort, healthcare costs, and the risk of complications such as infection, encrustation, and ureteral injury. Delayed or missed removals can lead to serious outcomes, including obstruction or kidney damage. Biodegradable stents are designed to degrade safely within the body after serving their function, thereby eliminating the need for retrieval. Over the past two decades, various biodegradable polymers, such as PLGA, PLA, PLLA, PCL, and PDLLA, have been used to make ureteral stents and evaluated in preclinical studies. While many early prototypes succeeded in providing temporary stenting, inconsistent degradation and local toxicity remain significant obstacles.[132] To address these challenges, Zhang *et al.* developed a stent composed of methoxypoly(ethylene glycol)-*block*-poly(L-lactide-ran-ε-caprolactone) (mPEG-*block*-PLACL), which demonstrated increased hydrophilicity and controlled degradation *in vitro*. In a 7-day dynamic urine circulation model, this material suppressed calcium and Mg encrustation. *In vivo* evaluation in rats showed significantly reduced mucosal hyperplasia (~29% in mPEG-PLACL *vs.* ~100% in control) and 71% calcium and 92% Mg reduction after 7 weeks.[133] Barros *et al.* fabricated a gelatin/alginate-based stent (HydrUStent™) using supercritical CO_2 processing. It degraded fully in 10 days in

porcine ureters and exhibited superior biocompatibility and mechanical performance, with lower encrustation and bacterial adhesion than a commercial polymer stent.[134] Additionally, biodegradable metallic stents have also been investigated to offer enhanced structural support compared to polymeric stents. For instance, Tie *et al.* developed and implanted ZJ41 Mg alloy (Mg–4Zn–1Sr, mass%) stents in pigs, which maintained shape integrity for 7 weeks and achieved complete degradation by 12 weeks (Fig. 6e).[135] The ZJ41 Mg alloy demonstrated better bacterial resistance than that of stainless steel (Fig. 6f), and PET-CT imaging showed no inflammation or tissue damage over 14 weeks. While these biodegradable platforms successfully address the issue of stent retrieval and show potential for passively reducing complications, they do not offer active therapeutic capabilities, such as inhibiting tumor growth, preventing inflammation, or actively dissolving stones. This limitation highlights the need for the next evolution in stent technology: drug-eluting stents designed to actively modulate the local biological environment.

5.2.6. Drug-eluting ureteral stents. To actively combat the primary causes of ureteral stent failure, DESs have been developed to provide sustained, localized delivery of therapeutic agents. The therapeutic strategy for ureteral DES is multifaceted, directly addressing the unique challenges of the urinary tract. The primary and most critical goal is to prevent or disrupt bacterial biofilm formation and subsequent encrustation, often using antibiotics, antiseptics, or novel antimicrobial agents. Secondary yet significant objectives include mitigating the host's inflammatory response to alleviate stent-related pain and discomfort, and, in specific cases of ureteral stricture, inhibiting fibroblast proliferation to prevent restenosis. This approach targets the key pathological processes of bacterial infection, encrustation, inflammation, and cellular hyperplasia directly at the stent-tissue interface.[136]

A major focus of ureteral DES has been the prevention of urinary tract infections (UTIs) and subsequent encrustation. Stents have been coated with a variety of broad-spectrum antibiotics and antiseptics. For example, triclosan-eluting stents demonstrated effective inhibition of common uropathogens like *P. mirabilis* and *E. coli* in preclinical models, though clinical trial results were less conclusive.[137] To address the risk of antibiotic resistance, alternative strategies are being explored. Nitric oxide (NO)-releasing catheters have shown broad-spectrum bactericidal properties and an ability to prevent biofilm formation without inducing resistance.[138,139] Another approach involves bio-inspired coatings, such as a polydopamine layer coordinated with copper ions and antimicrobial peptides (AMPs), which effectively suppresses bacterial growth and biofilm formation *in situ*.[140–143]

Beyond infection, DES are also designed to mitigate the host's inflammatory and proliferative responses. To alleviate stent-related pain and discomfort, stents have been coated with nonsteroidal anti-inflammatory drugs (NSAIDs) like ketorolac, which demonstrated significant pain reduction in a randomized clinical trial involving 276 patients.[144] For preventing ureteral strictures caused by excessive fibroblast proliferation and collagen deposition, stents eluting anti-proliferative agents such as paclitaxel and rapamycin have been developed. For example, a rapamycin-eluting bilayered degradable stent made of poly(lactic-*co*-glycolic acid) and polycaprolactone effectively inhibited fibrosis-related protein expression (TGF-β1 and α-SMA) in a rat model of ureteral injury.[145] In another approach, a trilayered biodegradable stent released both paclitaxel and rapamycin from silk fibroin layers, which significantly inhibited the proliferation of smooth muscle cells and fibroblasts *in vitro* and showed good biocompatibility in rat models.[146] For treating upper tract urothelial carcinoma (UTUC), stents loaded with chemotherapeutic agents like mitomycin C have been investigated. A biodegradable stent coated with silk fibroin and loaded with mitomycin C demonstrated a controlled release over 12 hours, though animal studies revealed challenges with ureteric strictures and obstructive stent fragments.[147,148]

Despite extensive preclinical research and promising results, the clinical translation of ureteral DES remains in its early stages. A significant challenge is designing a drug delivery platform that can provide sustained release over weeks to months in the highly dynamic and corrosive urinary environment.[136] The rapid flow of urine can wash away drugs, and the coating itself must resist degradation and encrustation to function correctly. Furthermore, while numerous animal studies have demonstrated proof-of-concept, there is a stark lack of human clinical trials, and currently, no drug-eluting ureteral stent is commercially available.[136] Establishing the long-term safety, particularly concerning local tissue toxicity and the effects of drug byproducts, and proving definitive clinical efficacy in large, randomized trials are critical hurdles that must be overcome before these advanced stents can become a standard of care.[149]

6. Eye stents

6.1. Glaucoma and treatments

Glaucoma is a group of ocular disorders characterized by optic nerve damage and irreversible visual loss. The condition is typically caused by impaired drainage of aqueous humor, leading to increased intraocular pressure (IOP) (Fig. 7a). In 2020, approximately 76 million individuals worldwide were affected, a number projected to rise to nearly 112 million by 2040, with over 3 million currently living with glaucoma in the U.S.[150] Because glaucoma often remains asymptomatic until advanced stages, only 10–50% of those affected are aware of their condition.[151] Primary open-angle glaucoma (POAG) accounts for over 80% of cases, while the remaining cases are predominantly angle-closure glaucoma. The hallmark of POAG is an elevated IOP (>21 mm_{Hg}), driven by impaired aqueous humor outflow.

Current treatments for POAG focus exclusively on lowering IOP. Topical medications (*e.g.*, prostaglandin analogs) are first-line due to their non-invasive nature, though irritation affects up to 40% of patients, and poor long-term adherence and cost

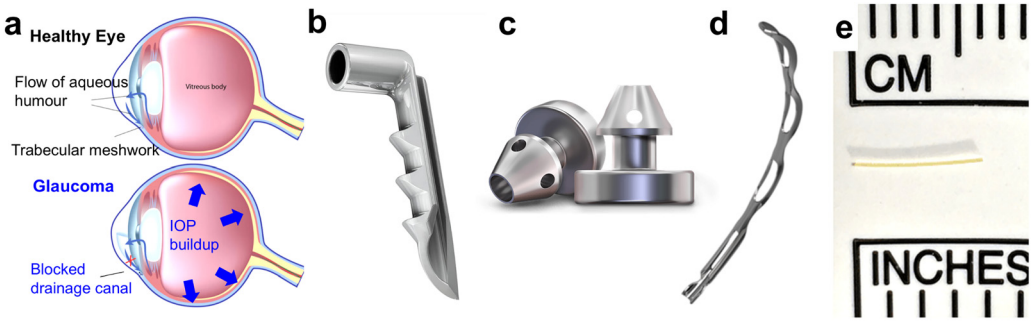

Fig. 7 (a) Glaucoma. The image was adapted from Fort Worth Eye Associates. (b) iStent™ (Glaukos Corporation). (c) iStent Inject® (Glaukos Corporation) with 2 stents per device and each with 4 lateral outlet lumens for multidirectional outflow. (d) The Hydrus™ Microstent (Ivantis, Alcon). (e) XEN™ Gel stent (Allergan).

issues are common.[152] When medications are insufficient, selective laser trabeculoplasty (SLT) is typically the next step: it uses low-energy lasers to enhance trabecular meshwork outflow, lowering IOP by 30%, with a 6- to 12-month success rate of 55–82%.[153] While SLT efficacy wanes over time, success rates drop to roughly 50% at 3 years and 32% at 5 years.[154] For advanced or refractory cases, surgical trabeculectomy creates a new drainage pathway and offers sustained IOP reduction, but comes with a 37–50% failure rate due to complications such as persistent hypotony and vision loss.[155]

6.2. Challenges for eye stents in the ocular microenvironment

Over the past decade, minimally invasive glaucoma surgeries (MIGS) have emerged as a promising approach to effectively treat glaucoma *via* the ab-interno or ab-externo approaches for lowering IOP with minimal or no scleral dissection. MIGS effectively lower IOP by implanting micro-stents that enhance aqueous humor outflow *via* Schlemm's canal or the subconjunctival space.[156] These micro-stents are tiny, typically 45–140 μm in diameter and 1–8 mm in length, depending on the device. Their performance is related to the unique microscale, pressure-driven biomechanical environments of the anterior chamber. First, the ability to modulate outflow resistance is critical for eye stents. In glaucomatous eyes, the increased outflow resistance arises primarily from pathological alterations in the juxtacanalicular trabecular meshwork and the inner wall of Schlemm's canal.[157,158] Devices such as the iStent™ and Hydrus™ must therefore be designed to bypass or support these delicate micron-level structures without inducing mechanical trauma. Second, given the natural fluctuations of IOP,[159–161] micro-stents must maintain structural stability under variable pressure gradients while remaining sufficiently compliant to avoid damaging adjacent tissues. Third, long-term stent failure is frequently caused by fibrosis, particularly bleb scarring in subconjunctival drainage procedures, which progressively blocks the outflow pathway and restores pathological resistance.[162] These challenges have motivated the development of diverse material compositions, geometries, and surface modifications in commercial MIGS devices to achieve precise flow control, mechanical compatibility, and improved resistance to fibrosis.

6.3. Commercial MIGS devices and associated challenges

These devices are designed to create or enhance aqueous humor outflow pathways through a permanent physical scaffold, representing the traditional MIGS approach. They are further classified by their target outflow pathway.

6.3.1. Permanent mechanical stents. iStent™ (Glaukos; FDA-approved in 2012). The first generation iStent is a heparin-coated, Ti trabecular bypass stent implanted into Schlemm's canal to bypass the trabecular meshwork (Fig. 7b). Studies involving combined cataract and iStent surgery have reported ~42% IOP reduction and up to 91% of patients achieving ≥28% IOP reduction (≤18 mm_{Hg}) without additional therapy for 3 years.[163] Although the iStent is commonly implanted with concurrent cataract surgery, clinical evidence also demonstrated that iStent implantation as a standalone procedure could result in a significant reduction in IOP and in the dependency on glaucoma medications.[164] In 2018, the second generation iStent, iStent Inject® (Fig. 7c), was introduced to further improve their clinical performance. iStent Inject delivers two stents in a single entry into the eye, offering an increased surface area for aqueous humor outflow and further enhancing the reduction of IOP.[165]

Hydrus™ Microstent (Alcon; FDA-approved in 2018). The Hydrus is a nitinol stent designed to enhance outflow by dilating and scaffolding a portion of Schlemm's canal (Fig. 7d). Made from nitinol, its superelastic properties allow it to be delivered flexibly and then self-expand to gently support the canal's structure over a length of 8 mm.[166] Clinical data showed that the Hydrus microstent had a higher surgical success rate (*e.g.* 35.6% *vs.* 10.5% 12-month cumulative event-free survival rate) and greater medication reduction (*e.g.* 46.6% *vs.* 24.0% medication free) compared to the iStent.[167] Five-year clinical trial results demonstrated that Hydrus microstent implantation effectively lowered IOP, reduced the need for medication use, and decreased the likelihood of postoperative incisional glaucoma filtration surgery compared to cataract surgery alone after 5 years, without adversely affecting the corneal endothelium.[166] While the Hydrus microstents show promising results, more long-term follow-up studies are needed to assess the durability of its effects.

XEN Gel stent (Allergan; FDA-approved in 2016). XEN Gel stent is a hydrophilic tube made of porcine collagen cross-linked with glutaraldehyde (Fig. 7e). Unlike the iStent and Hydrus, which aim to enhance aqueous outflow *via* Schlemm's canal, the XEN Gel stent is designed to create a new outflow pathway from the anterior chamber to the subconjunctival space *via* an ab interno approach.[168,169] XEN Gel stents were tested in 64 patients with standalone implantation and those combined with cataract surgery over a 4-year period.[170] The study reported a 40% reduction in IOP and a 50% decrease in the use of glaucoma medications. However, an annual surgical failure rate of approximately 10% was observed, defined as the need for additional IOP-lowering procedures or loss of light perception. Another study analyzed the efficacy of the XEN Gel stent from 78 studies published before May 2021.[171] Their analysis confirmed that the XEN Gel stent is effective in IOP reduction and reduction in medication utilization. However, XEN Gel stent implantation is associated with a relatively high needling rate, particularly when used as a standalone procedure. Reported needling rates ranged from 35.6% to 48.6% for standalone implantation, compared to 34.8% when combined with cataract surgery and 19% following trabeculectomy. The primary reason for needling is bleb fibrosis or scar formation, which can directly obstruct the stent and compromise its function, underscoring the central challenge of subconjunctival implants.

6.3.2. Biodegradable, drug-eluting implants. A newer class of glaucoma implants shifts treatment from purely mechanical aqueous humor drainage to sustained, implant-based drug delivery, directly addressing the major clinical challenge of patient non-adherence to topical medications. These systems may be biodegradable or permanent, and deliver long-acting prostaglandin analogs to achieve continuous IOP reduction.

Durysta® (Allergan; FDA-approved in 2020). Durysta® is a biodegradable intracameral implant approved for sustained drug delivery in glaucoma. The cylindrical implant (diameter of 200 μm, length of 1.1 mm) is composed of PLGA polymers and contains 10 μg of bimatoprost, which is released in a continuous, nonpulsatile manner for approximately 3–4 months.[172] Its biodegradable nature offers two key advantages in mitigating fibrosis. First, as the implant fully degrades, it removes the chronic mechanical signal that typically drives subconjunctival or intracameral fibrosis around permanent implants. Second, high local drug concentrations may modulate extracellular matrix turnover by upregulating MMP1 and downregulating fibronectin to enhance aqueous outflow and sustain the IOP-lowering effect after drug depletion.[173] Durysta® markedly improves therapeutic adherence and reduces topical medication burden in real-world studies. However, a major limitation is its FDA approval for single administration per eye, due to concerns about cumulative corneal endothelial cell loss with repeated dosing.[174]

iDose® TR (Glaukos; FDA-approved in 2023). iDose TR is a permanent, titanium-based, drug-eluting implant placed through the trabecular meshwork and anchored in the sclera. The device contains a reservoir of travoprost, sealed with a proprietary membrane to provide controlled, long-term drug diffusion directly into the anterior chamber.[175] This approach enables continuous drug delivery independent of patient adherence. In a real-world series of standalone implantations, iDose TR achieved a 33.2% reduction in mean IOP at 3 months, with 100% of eyes becoming drop-free.[176] This system exemplifies the emerging paradigm of ''interventional glaucoma'', shifting therapy from patient-dependent topical regimens to reliable, long-acting implants.

6.4. Limitations and future directions in eye stents and implants

Despite meaningful advances, current devices have important limitations. Trabecular bypass stents such as iStent™ and Hydrus™ have excellent safety profiles but typically achieve only modest IOP reductions, making them more suitable for mild-to-moderate disease. Subconjunctival implants like the XEN Gel stent face the persistent challenge of bleb fibrosis, often necessitating postoperative needling or revision procedures.[177] Durysta®, while avoiding the long-term foreign body response, is limited by its single-use restriction and concerns regarding corneal endothelial safety upon re-dosing. These issues highlight the need for materials with both long-term biocompatibility and repeated-administration safety. To overcome the shortcomings of topical medications, including poor adherence and ocular surface toxicity, a new class of procedural pharmaceuticals or drug-eluting implants has emerged. Unlike drug-eluting stents in other luminal systems, which aim to prevent restenosis or infection, glaucoma drug-eluting implants primarily seek to replace patient-administered therapy entirely by functioning as long-lived drug reservoirs. Future innovation will likely focus on developing materials for reusable or refillable drug depots, biodegradable implants optimized for safe repeated administration, and hybrid systems integrating mechanical outflow enhancement with controlled pharmacologic therapy.

7. Other stents for treating NVLDs

7.1. Biliary stent

Biliary stricture refers to the abnormal narrowing of the bile duct, often resulting from malignancies, gallstone-related scarring, or iatrogenic injury during surgery. Such strictures can obstruct bile flow and impair digestion, potentially leading to complications, such as jaundice and cirrhosis.[178] Although surgical options such as hepaticojejunostomy or ductal resection offer definitive treatment for both benign and malignant strictures, these procedures are highly invasive and not suitable for all patients due to associated risks and comorbidities. As a less invasive alternative, biliary stent placement is widely used to relieve obstruction, restore bile flow, and support ductal remodeling. The biliary tract presents a harsh biochemical environment, where the constant flow of bile promotes the formation of bacterial biofilms and sludge accumulation, making stent occlusion a primary mode of failure. In addition, the

relaxation of the sphincter and ductal dilation reduce frictional anchoring, resulting in stent migration into the duodenum, common bile duct, or the colon.[179]

Currently, biliary stents are typically fabricated from either metallic or plastic materials. Common metallic biliary stents are made of nitinol, such as WallFlex™ (Boston Scientific), HANAROSTENT® (OLYMPUS), and Niti-S™ D (Taewoong Medical). Some metallic stents, like WallFlex™, are partially or fully coated with silicone or other polymers to reduce tissue ingrowth, which is a major complication that can lead to stent occlusion.[180] Plastic stents are commonly made from materials such as polypropylene (*e.g.*, Advanix™, Boston Scientific) or polyethylene (*e.g.*, Cotton-Leung®, Cook Medical). Their high efficacy, ease of insertion and removal, and relatively low-cost result in broad clinical adoption. However, a major limitation of plastic stents is their high susceptibility to occlusion, which is primarily due to bacterial biofilm formation. This can result in recurrent jaundice, pruritus, and other complications. Notably, acute cholangitis has been reported in 20–40% of cases, often requiring stent exchange or additional surgical intervention to restore biliary drainage.[181]

To overcome these limitations and eliminate the need for secondary removal surgery, biodegradable biliary stents have been developed. Clinical studies demonstrated the safety and effectiveness of poly-*p*-dioxanone (PDO)-based stents (PDX, ELLA-CS).[182] The main drawbacks of PDX stents are their relatively low mechanical strength, which limits their application in complex biliary structures. PLLA stents were able to maintain superior mechanical strength during the degradation process in bile.[183] Moreover, PLLA appeared to reduce long-term sludge accumulation due to the surface degradation, potentially addressing a key challenge for biliary stent patency.[184]

In addition to biodegradable polymers, biodegradable metals, particularly Mg alloys, have emerged as a promising alternative for biliary stents. Mg alloys offer superior initial mechanical strength and exhibit intrinsic bioactivity that may provide therapeutic benefits. A major challenge, however, is their rapid corrosion in physiological environments.[185] To address this, various surface-modification strategies have been developed. Fluoride treatments and biodegradable polymer coatings form temporary protective barriers that significantly reduce early corrosion and hydrogen evolution, thereby prolonging the period during which Mg stents maintain clinically meaningful mechanical integrity.[186,187] In addition, alloy design has also been instrumental in achieving controlled corrosion and improved biocompatibility. For example, Mg–6Zn alloys demonstrated an appropriate *in vivo* degradation rate ($\sim$0.107 mm per year) and did not induce significant apoptosis in surrounding tissues when implanted in the rabbit common bile duct for three weeks, supporting their suitability as biodegradable biliary stents.[188,189] Similarly, WE43 alloys exhibited slower corrosion in human bile compared with pure Mg.[190] Beyond mechanical and corrosion behavior, emerging evidence suggests that Mg degradation products may exert anti-tumor effects. *In vitro* evaluation and xenograft tumor models showed that Mg-based materials can inhibit gallbladder cancer cell proliferation,[191] further supporting their potential in biliary applications. Notably, UNITY-B, a balloon-expandable Mg alloy stent (MgNdMn21) with a polymer surface coating, has received CE certification, although detailed clinical performance data remain limited.[192]

Building on the concept of bioactive materials, drug-eluting stents (DES) have been developed to directly address the dominant biological causes of stent failure. In malignant biliary strictures, DES are primarily designed to deliver local chemotherapy. Stents incorporating paclitaxel (PTX) or gemcitabine (GEM) have demonstrated effective inhibition of tumor ingrowth in both preclinical models and early clinical studies.[193,194] For instance, a PTX-eluting covered metallic stent achieved a mean patency of 429 days in patients with malignant biliary obstruction, a substantial improvement over non-eluting covered stents.[195] Antibacterial coatings incorporating silver nanoparticles have also shown strong anti-biofilm activity, addressing one of the major causes of occlusion in plastic biliary stents.[196,197]

7.2. Colonic stent

Colorectal cancer is the second leading cause of cancer-related deaths in the United States.[198] Malignant colonic obstruction occurs in approximately 10–40% of these patients, presenting with symptoms such as nausea, vomiting, abdominal pain, and severe distension.[199] While emergency surgery remains the standard treatment, it is not suitable for all patients and carries a high risk of morbidity and mortality.[200] As a less invasive alternative, colonic stent placement has been widely adopted as a ''bridge to surgery'' (BTS). By relieving the obstruction and decompressing the bowel, stents allow time for medical optimization and elective tumor resection under improved conditions, thereby reducing surgical complications and mortality. Current colonic stents are self-expanding nitinol stents, such as Wallflex™ (Boston Scientific), Evolution™ (Cook Medical), and ComVi™ (TaeWoong Medical). Studies have shown that stent placement followed by elective surgery is associated with shorter hospital stays, fewer procedures, and reduced ICU time compared to emergency surgery.[200]

However, the use of colonic stents faces challenges due to the complex mechanical and biological environment of the large intestine. The colon's tortuous geometry and strong segmental peristalsis impose substantial radial and axial stresses on implanted devices, contributing to a high incidence of stent migration and, more critically, perforation.[201–203] In addition, the colon contains a dense polymicrobial community and a solid fecal stream, creating an environment unlike any other non-vascular lumens and introducing distinct risks of infection, biofilm formation, and mechanical obstruction.[204] Perforation is particularly concerning, as it may facilitate tumor cell dissemination and has been associated with increased rates of locoregional recurrence in patients with malignant obstruction.[205,206] To address tumor ingrowth through the mesh of uncovered nitinol stents, covered stents were introduced. While these effectively reduce tumor ingrowth, their

smooth surfaces prevent tissue embedding, resulting in markedly higher migration rates.[207–209]

To overcome the limitations of permanent metallic stents, BDSs made from polymers, such as PDO, have been investigated. The primary advantage of BDSs is that they provide temporary luminal support and then degrade, obviating the need for a second procedure for removal, which is a significant benefit in benign strictures or temporary applications.[210] However, their clinical translation in the colon has been challenging. BDSs generally exhibited lower radial force compared to nitinol SEMS, and their degradation behavior can be unpredictable in the complex colonic environment.[210] Moreover, current BDS delivery systems are often insufficiently long or flexible for placement in the proximal colon, restricting their use largely to distal lesions.[211]

The development of DESs represents a more targeted strategy aimed at modifying the local biological response. In malignant obstruction, neoadjuvant chemotherapy (NAC) is commonly administered systemically after SEMS placement. This ''SEMS-NAC'' approach has been shown to improve nutritional status, increase lymph-node harvest, and potentially enhance overall survival by treating micrometastatic disease during the bridging period.[212,213] While fully developed colonic DES capable of sustained local chemotherapy are still in early stages, their therapeutic rationale is clear: delivering cytotoxic agents directly to the tumor site to improve local control and optimize outcomes of subsequent surgery. The central challenge is designing drug-release systems that remain stable and functional within the harsh enzymatic and microbiota-rich environment of the colon.[214] While promising concepts exist for other parts of the GI tract, such as radioactive stents loaded with iodine-125 seeds for esophageal and biliary cancers, and paclitaxel-eluting stents studied for malignant biliary obstruction, robust clinical data for DESs specifically engineered for colonic malignancies are still lacking.[103,215–217]

8. Overall comparison of stents for various NVLDs

The comparison of stents used across various NVLDs (Table 3) reveals a clear dichotomy driven by differences in luminal biomechanics and biology. In high-force environments such as the esophagus and airway, stent migration and loss of mechanical integrity are dominant challenges due to strong peristalsis and respiratory deformation. In contrast, biological complications are more prevalent in less dynamic lumens, including biofilm formation and encrustation in the urethra, and fibrosis associated with eye and biliary stents. This divergence highlights the limitations of relying on uniform material strategies and underscores the need for organ-specific, bioactive stent platforms engineered to address the distinct pathophysiological demands of each luminal system.

Table 3 Overall comparison of stents used across various NVLDs

Application	Clinical challenge	Common materials	Main failure modes	Key features in degradation or drug eluting
Airway	Dynamic compression, mucus plugging	Silicone, nitinol	Migration: ~25% (silicone) Granulation: 16% (silicone) *vs.* 57% (bare metal) Blockage: ~24% (silicone)	BDS: PDO stents degrade in weeks; 3D-printed PLLA-*co*-PCL mimics silicone mechanics. DES: Sirolimus/paclitaxel DES at preclinical stage.
Esophagus	High-amplitude peristalsis, tumor ingrowth	Nitinol, PU	Migration: 6.5% (BDS) *vs.* 23–31% (covered SEMS) *vs.* 47–67% (plastic) Chest pain: ~10–14% Tumor ingrowth: ~17–36% (uncovered SEMS)	BDS: PDO (SX-ELLA) degrades in 9–12 weeks; coated Mg-alloys for controlled degradation. DES: paclitaxel/radioactive I-125 for malignant strictures.
Ureter	Biofilm/encrustation, frictional irritation	Silicone, PU	Infection/encrustation: affects >80% of patients Pain/discomfort	BDS: ZJ41 Mg-alloy fully degrades by 12 weeks with antibacterial properties. DES: ketorolac (pain); antibiotics/NO (anti-infection) at investigational stage.
Eye	Bleb fibrosis, micro-scale flow control	Ti, nitinol, collagen	Fibrosis (requiring needling: ~35–49%) Hypotony, migration	Permanent DES: iDose® TR (Ti) serving as a long-term travoprost reservoir. BDS/DES: Durysta® degrades in ~90 days, avoiding chronic foreign body response.
Biliary duct	Biofilm/sludge occlusion, tumor ingrowth	Nitinol, polypropylene	Occlusion: primary failure mode Cholangitis: 20–40%	BDS: PDO stents in clinical use; coated Mg-alloy (UNITY-B) is CE-marked. DES: paclitaxel/gemcitabine for malignancy; AgNP coatings for anti-infection.
Colon	High peristalsis, high perforation risk	Nitinol	Perforation: major safety concern Migration: higher risk with covered stents	BDS: limited use due to weak radial force and delivery system constraints. DES: no dedicated colonic DES; strategy is ''stent + neoadjuvant chemotherapy''.

9. Conclusion and future directions

Stent technology, originally developed for coronary interventions, has since been adapted for a wide range of NVLDs, including those affecting the airway, esophagus, ureter, ocular outflow tract, biliary system, and colon. Despite their clinical utility, the translation of advanced stent concepts into non-vascular applications has progressed slowly compared with vascular stents. This review has summarized the distinct pathophysiological conditions across NVLDs and highlighted current clinical devices and emerging technologies. Several key challenges must be addressed to enable broader clinical adoption.

Material limitations remain a major barrier for the development of biodegradable stents. Biodegradable polymers such as PLLA, PLGA, and PCL often lack the radial strength required to maintain patency in mechanically demanding lumens, whereas magnesium-based alloys, though mechanically robust, frequently degrade too rapidly or unpredictably. Degradation byproducts, particularly acidic products from polyester-based stents, can further exacerbate inflammation or impair healing. Achieving a balance between mechanical durability and predictable degradation remains difficult, especially because surface treatments or reinforcement strategies may inadvertently accelerate corrosion or alter hydrolysis kinetics. Future efforts should focus on the exploration of new polymer chemistry, such as citrate-based polymers,[16,37] composite systems that combine polymer flexibility with metallic strength, surface-engineered Mg alloys with controlled corrosion, and bioactive coatings that promote tissue integration while minimizing inflammatory responses.

Drug-eluting strategies offer considerable promise but require organ-specific optimization. Whereas coronary DES primarily target the inhibition of smooth muscle proliferation, non-vascular lumens impose different biological challenges, including fibrosis (airway, esophagus), biofilm formation and encrustation (ureter), or scarring of subconjunctival tissues (glaucoma). Tailoring drug selection, dosage, and release kinetics to each luminal microenvironment remains a significant challenge. Advanced platforms, such as stimuli-responsive polymers, nano-reservoir systems, or spatiotemporally controlled drug-eluting architectures, may enable more precise modulation of local tissue responses.

Translation to clinical practice is further hindered by gaps in regulation, manufacturing, and long-term evaluation. Robust randomized clinical trials are limited for most non-vascular stent technologies, and regulatory pathways for combination products (particularly biodegradable, drug-eluting devices) remain complex. Manufacturing challenges, such as ensuring reproducible degradation behavior, maintaining lot-to-lot consistency, and validating internal architecture with non-destructive testing, must be addressed before widespread adoption. In parallel, long-term safety data addressing the systemic impacts of degradation products and chronic local drug exposure remain essential.

In addition, given the substantial variability in patient anatomy and disease presentation, patient-specific stents enabled by advances in high-resolution imaging and additive manufacturing represent a promising direction. The integration of biosensors capable of monitoring local inflammation, patency, or mechanical loading could enable next-generation ''smart stents'' that autonomously adjust drug release or provide early warnings of device failure. In summary, the future of non-vascular stenting will rely on coordinated progress in materials engineering, drug delivery, device manufacturing, and clinical investigation. By addressing the unique biomechanical and biological challenges of each luminal environment and leveraging emerging technologies in biomaterials, controlled drug release, and personalized manufacturing, the field is well positioned to advance toward safer, more effective, and durable solutions for the minimally invasive treatment of occlusive luminal diseases.

Conflicts of interest

There are no conflicts to declare.

Data availability

This is a review article. No primary research results, software or code have been included and no new data were generated or analysed as part of this review.

Acknowledgements

This work was supported by American Heart Association Career Development Award (AHA, Grant: 852772) to Y. Ding.

References

1 Y. Zhu, K. Yang, R. Cheng, Y. Xiang, T. Yuan, Y. Cheng, B. Sarmento and W. Cui, *Mater. Today*, 2017, **20**, 516–529.
2 H. Y. Ang, H. Bulluck, P. Wong, S. S. Venkatraman, Y. Huang and N. Foin, *Int. J. Cardiol.*, 2017, **228**, 931–939.
3 C. Pan, Y. Han and J. Lu, *Micromachines*, 2021, **12**, 770.
4 S. H. Im, D. H. Im, S. J. Park, Y. Jung, D.-H. Kim and S. H. Kim, *Prog. Mater. Sci.*, 2022, **126**, 100922.
5 M. Ullah, A. Wahab, S. U. Khan, U. Zaman, K. ur Rehman, S. Hamayun, M. Naeem, H. Ali, T. Riaz and S. Saeed, *Curr. Probl. Cardiol.*, 2023, **48**, 101415.
6 N. Beshchasna, M. Saqib, H. Kraskiewicz, Ł. Wasyluk, O. Kuzmin, O. C. Duta, D. Ficai, Z. Ghizdavet, A. Marin and A. Ficai, *Pharmaceutics*, 2020, **12**, 349.
7 D. Stoeckel, A. Pelton and T. Duerig, *Eur. Radiol.*, 2004, **14**, 292–301.
8 S. Robertson, A. Pelton and R. Ritchie, *Int. Mater. Rev.*, 2012, **57**, 1–37.
9 B. D. Vermeulen and P. D. Siersema, *Curr. Treat. Options Gastroenterol.*, 2018, **16**, 260–273.
10 A. Tringali, C. Hassan, M. Rota, M. Rossi, M. Mutignani and L. Aabakken, *Endoscopy*, 2018, **50**, 631–641.

11 E. J. Kim and Y. J. Kim, *World J. Gastroenterol.*, 2016, **22**, 842.
12 Q. Wang, R. Wang, Z. Ye, J. Chen, Y. Xu, W. Ye, S. Li and Y. Chen, *Respirology*, 2025, **30**, 751–759.
13 S. Lyu and D. Untereker, *Int. J. Mol. Sci.*, 2009, **10**, 4033–4065.
14 A. Kirillova, T. R. Yeazel, D. Asheghali, S. R. Petersen, S. Dort, K. Gall and M. L. Becker, *Chem. Rev.*, 2021, **121**, 11238–11304.
15 S. McMahon, N. Bertollo, E. D. O'Cearbhaill, J. Salber, L. Pierucci, P. Duffy, T. Dürig, V. Bi and W. Wang, *Prog. Polym. Sci.*, 2018, **83**, 79–96.
16 H. Wang, S. Huddleston, J. Yang and G. A. Ameer, *Adv. Mater.*, 2024, **36**, 2306326.
17 L. N. Woodard and M. A. Grunlan, *ACS Macro Lett.*, 2018, **7**, 976–982.
18 K. Dodzi Lelkes, D. Jezbera, R. Svoboda, Š. Podzimek, J. Loskot, M. Nalezinková, P. Voda, P. Duda, A. Myslivcová Fučíková, T. Hosszú, D. Alferi and A. Bezrouk, *Polym. Test.*, 2024, **138**, 108536.
19 L. Xu, X. Liu, K. Sun, R. Fu and G. Wang, *Materials*, 2022, **15**, 2613.
20 J. Wang, Y. He, M. F. Maitz, B. Collins, K. Xiong, L. Guo, Y. Yun, G. Wan and N. Huang, *Acta Biomater.*, 2013, **9**, 8678–8689.
21 E. Zhang and F. Shen, *Mater. Sci. Eng., C*, 2015, **52**, 37–45.
22 T. He, X.-H. Liu, Z.-J. Xiao, Y.-L. Dai, Y.-C. Dou, J. She, L.-W. Lu, Y. Yang, L.-F. Wang, N. Zhao, W.-W. Wei, F.-G. Qi and X.-P. Ouyang, *Rare Met.*, 2025, **44**, 6730–6747.
23 L. Li, Z. Zhang, D. Zhang, F. Qi, Y. Dai, W. Wei and X. Ouyang, *J. Magnesium Alloys*, 2025, **13**, 296–310.
24 J. Lin, Y. Chen, Y. Dai, X. Zhang, D. Zhang, Y. Li and C. Wen, *Acta Biomater.*, 2025, **194**, 514–529.
25 W. Jiang, W. Zhao, T. Zhou, L. Wang and T. Qiu, *Micromachines*, 2022, **13**, 140.
26 E. García-López, A. G. Medrano-Tellez, J. R. Ibarra-Medina, H. R. Siller and C. A. Rodriguez, *Micromachines*, 2017, **9**, 4.
27 F. Ahlhelm, R. Kaufmann, D. Ahlhelm, M. F. Ong, C. Roth and W. Reith, *Cardiovasc. Interventional Radiol.*, 2009, **32**, 1019–1027.
28 T. Zou, L. Wang, W. Li, W. Wang, F. Chen and M. W. King, *J. Mech. Behav. Biomed. Mater.*, 2014, **38**, 17–25.
29 A. G. Demir and B. Previtali, *Mater. Des.*, 2017, **119**, 338–350.
30 V. Finazzi, A. G. Demir, C. A. Biffi, C. Chiastra, F. Migliavacca, L. Petrini and B. Previtali, *Procedia Struct. Integr.*, 2019, **15**, 16–23.
31 S. A. Park, S. J. Lee, K. S. Lim, I. H. Bae, J. H. Lee, W. D. Kim, M. H. Jeong and J.-K. Park, *Mater. Lett.*, 2015, **141**, 355–358.
32 S. K. Misra, F. Ostadhossein, R. Babu, J. Kus, D. Tankasala, A. Sutrisno, K. A. Walsh, C. R. Bromfield and D. Pan, *Adv. Healthcare Mater.*, 2017, **6**, 1700008.
33 S. J. Lee, H. H. Jo, K. S. Lim, D. Lim, S. Lee, J. H. Lee, W. D. Kim, M. H. Jeong, J. Y. Lim and I. K. Kwon, *Chem. Eng. J.*, 2019, **378**, 122116.
34 V. Chausse, R. Schieber, Y. Raymond, B. Segry, R. Sabate, K. Kolandaivelu, M.-P. Ginebra and M. Pegueroles, *Addit. Manuf.*, 2021, **48**, 102392.
35 R. Van Lith, E. Baker, H. Ware, J. Yang, A. C. Farsheed, C. Sun and G. Ameer, *Adv. Mater. Technol.*, 2016, **1**, 1600138.
36 H. Ware, Y. Ding, C. Collins, B. Akar, N. Akbari, H. Wang, C. Duan, G. Ameer and C. Sun, *Mater. Today Chem.*, 2022, **26**, 101231.
37 Y. Ding, L. Warlick, M. Chen, E. Taddese, C. Collins, R. Fu, C. Duan, X. Wang, H. Ware and C. Sun, *Bioact. Mater.*, 2024, **38**, 195–206.
38 E. L. Melgoza, G. Vallicrosa, L. Serenó, J. Ciurana and C. A. Rodríguez, *Rapid Prototyping J.*, 2014, **20**, 2–12.
39 Y. Wang, J. Xia, Z. Luo, H. Yan, J. Sun and E. Lü, *Addit. Manuf.*, 2020, **36**, 101506.
40 J. C. Hutchinson, S. C. Shelmerdine, I. C. Simcock, N. J. Sebire and O. J. Arthurs, *Br. J. Radiol.*, 2017, **90**, 20170113.
41 V. Pathak, R. W. Shepherd and S. Shojaee, *J. Thorac. Dis.*, 2016, **8**, 3818–3825.
42 R. Farzanegan, B. Farzanegan, M. Zangi, M. Golestani Eraghi, S. Noorbakhsh, N. Doozandeh Tabarestani and M. B. Shadmehr, *Iran. Red Crescent Med. J.*, 2016, **18**, e37574.
43 M. N. Samano, H. Minamoto, E. Q. Oliveira, M. L. Caramori, P. M. Pego-Fernandes and F. B. Jatene, *Clinics*, 2007, **62**, 643–644.
44 A. D'Andrilli, F. Venuta and E. A. Rendina, *J. Thorac. Dis.*, 2016, **8**, S140.
45 H. G. Auchincloss and C. D. Wright, *J. Thorac. Dis.*, 2016, **8**, S160.
46 A. Ratnovsky, N. Regev, S. Wald, M. Kramer and S. Naftali, *Med. Eng. Phys.*, 2015, **37**, 408–415.
47 S. K. Avasarala, L. Freitag and A. C. Mehta, *Chest*, 2019, **155**, 1246–1259.
48 E. Folch and C. Keyes, *Ann. Cardiothorac. Surg.*, 2018, **7**, 273–283.
49 J. Xu, H. X. Ong, D. Traini, M. Byrom, J. Williamson and P. M. Young, *Drug Dev. Ind. Pharm.*, 2019, **45**, 1–10.
50 S. Chen, T. Du, H. Zhang, Y. Zhang and A. Qiao, *Mater. Today Bio*, 2024, 101263.
51 N. Y. Madisi, D. Greenberg and A. Balwan, *Am. Med. J.*, 2024, **9**, DOI: 10.21037/amj-23-117.
52 J. Huang, Z. Zhang and T. Zhang, *J. Cardiothorac. Surg.*, 2018, **13**, 1–6.
53 J. Gottlieb, T. Fuehner, M. Dierich, O. Wiesner, A. Simon and T. Welte, *Eur. Respir. J.*, 2009, **34**, 1417–1422.
54 C. Dahlqvist, S. Ocak, M. Gourdin, A. S. Dincq, L. Putz and J.-P. d'Odémont, *Can. Respir. J.*, 2018, **2018**, 6202750.
55 S. Huang, J. Xu, Z. An, P. Yuan, H. Xu, W. Lv and J. Hu, *J. Thorac. Dis.*, 2018, **10**, 3277.
56 A. Ayub, A. M. Al-Ayoubi and F. Y. Bhora, *J. Thorac. Dis.*, 2017, **9**, S116.
57 E. Folch and C. Keyes, *Ann. Cardiothorac. Surg.*, 2018, **7**, 273.

58 L. Li, X. Zhang, J. Shi, Y. Chen, H. Wan, F. J. Herth and F. Luo, *Respiration*, 2023, **102**, 439–448.
59 E. M. Walser, *Eur. J. Radiol.*, 2005, **55**, 321–330.
60 D.-F. Chen, Y. Chen, C.-H. Zhong, X.-B. Chen and S.-Y. Li, *J. Thorac. Dis.*, 2021, **13**, 82.
61 H. S. Jung, G. Chae, J. H. Kim, C. Y. Park, S. Lim, S. E. Park, H. C. Kim, Y. J. Lee, S. K. Kang, D. H. Kim, Y. Lee and T. Lee, *Sci. Rep.*, 2021, **11**, 7958.
62 S. Rodriguez-Zapater, C. Serrano-Casorran, J. A. Guirola, S. Lopez-Minguez, C. Bonastre and M. A. de Gregorio, *Arch. Bronconeumol.*, 2020, **56**, 643–650.
63 N. Paunović, Y. Bao, F. B. Coulter, K. Masania, A. K. Geks, K. Klein, A. Rafsanjani, J. Cadalbert, P. W. Kronen and N. Kleger, *Sci. Adv.*, 2021, **7**, eabe9499.
64 S. Chen, T. Du, H. Zhang, Y. Zhang and A. Qiao, *Mater. Today Bio*, 2024, **29**, 101263.
65 M. Duvvuri, K. Motz, H.-W. Tsai, I. Lina, D. Ding, A. Lee and A. T. Hillel, *JoVE*, 2020, e60483, DOI: 10.3791/60483.
66 T. Wang, J. Zhang, J. Wang, Y. H. Pei, X. J. Qiu and Y. L. Wang, *Chin. Med. J.*, 2016, **129**, 2708–2713.
67 G. H. Zhu, A. H. C. Ng, S. S. Venkatraman, F. Y. C. Boey, A. L. Y. Wee, S. L. Trasti and L. H. Y. Lim, *Laryngoscope*, 2011, **121**, 2234–2239.
68 N. Maity, N. Mansour, P. Chakraborty, D. Bychenko, E. Gazit and D. Cohn, *Adv. Funct. Mater.*, 2021, **31**, 2108436.
69 H. Jung, J. S. Lee, J. J. Lee and H. S. Park, *In Vivo*, 2022, **36**, 1195–1202.
70 N. Guibert, H. Saka and H. Dutau, *Respirology*, 2020, **25**, 953–962.
71 K. Y. Kim, J. Tsauo, H.-Y. Song, P. H. Kim and J.-H. Park, *J. Korean Med. Sci.*, 2017, **32**, 1062.
72 T. Yuan, J. Yu, J. Cao, F. Gao, Y. Zhu, Y. Cheng and W. Cui, *Materials*, 2016, **9**, 384.
73 L.-L. Liu, J. Qin, C.-H. Zeng, R.-J. Du, T. Pan, J.-J. Ji, L.-G. Lu, L. Chen, D.-F. Liu and J. Yang, *Acta Biomater.*, 2022, **146**, 495–505.
74 A. Ruigómez, L. A. G. Rodríguez, M.-A. Wallander, S. Johansson and S. Eklund, *J. Am. Coll. Gastroenterol.*, 2006, **101**, 2685–2692.
75 S. F. Pasha, R. D. Acosta, V. Chandrasekhara, K. V. Chathadi, G. A. Decker, D. S. Early, J. A. Evans, R. D. Fanelli, D. A. Fisher and K. Q. Foley, *Gastrointest. Endosc.*, 2014, **79**, 191–201.
76 N. Khanna, *Can. J. Gastroenterol. Hepatol.*, 2006, **20**, 153–155.
77 M. M. C. Hirdes, F. P. Vleggaar, M. de Beule and P. D. Siersema, *Endoscopy*, 2013, **45**, 997–1005.
78 R. Ishihara, *Curr. Oncol.*, 2023, **30**, 5984–5994.
79 H. Iwagami, R. Ishihara, S. Yamamoto, N. Matsuura, A. Shoji, K. Matsueda, T. Inoue, M. Miyake, K. Waki, H. Fukuda, Y. Shimamoto, M. Kono, H. Nakahira, S. Shichijo, A. Maekawa, T. Kanesaka, Y. Takeuchi, K. Higashino and N. Uedo, *Sci. Rep.*, 2021, **11**, 2134.
80 M. Uesato, Y. Akutsu, K. Murakami, Y. Muto, A. Kagaya, A. Nakano, M. Aikawa, T. Tamachi, T. Arasawa, H. Amagai, Y. Muto and H. Matsubara, *Gastroenterol. Res. Pract.*, 2017, **2017**, 2560510.
81 G. L. Wu, G. H. Wei, S. H. Huang, Q. L. Zhang, S. Zeng, J. Feng, B. Zeng and P. Yu, *Front. Phys.*, 2024, **12**, 1390321.
82 N. Mbah, P. Philips, M. J. Voor and R. C. G. Martin, *Surg. Endosc.*, 2017, **31**, 5076–5082.
83 G. Diamantis, M. Scarpa, P. Bocus, S. Realdon, C. Castoro, E. Ancona and G. Battaglia, *World J. Gastroenterol.*, 2011, **17**, 144.
84 P. D. Siersema, *Gastroenterol. Hepatol.*, 2018, **14**, 189.
85 F. P. Vleggaar and P. D. Siersema, *Tech. Gastrointest. Endosc.*, 2010, **12**, 231–236.
86 A. L. Halpern and M. D. McCarter, *Surg. Clin.*, 2019, **99**, 555–569.
87 Y. Kang, *BioMed Res. Int.*, 2019, **2019**, 9265017.
88 S. Thomas, A. A. Siddiqui, L. J. Taylor, S. Parbhu, C. Cao, D. Loren, T. Kowalski and D. G. Adler, *Endosc. Int. Open*, 2019, **7**, E751–E756.
89 E. M. Verschuur, E. W. Steyerberg, E. J. Kuipers and P. D. Siersema, *Gastrointest. Endosc.*, 2007, **65**, 592–601.
90 Z. Hussain, A. Diamantopoulos, M. Krokidis and K. Katsanos, *World J. Gastroenterol.*, 2016, **22**, 7841.
91 M. Conio, A. Repici, G. Battaglia, G. De Pretis, L. Ghezzo, M. Bittinger, H. Messmann, J.-F. Demarquay, S. Blanchi and M. Togni, *J. Am. Coll. Gastroenterol.*, 2007, **102**, 2667–2677.
92 A. N. Holm, J. G. de la Mora Levy, C. J. Gostout, M. D. Topazian and T. H. Baron, *Gastrointest. Endosc.*, 2008, **67**, 20–25.
93 T. Wang, H. Cui, Y. Shao, H. Jiang, Y. Dong and R. Guo, *Int. J. Clin. Exp. Med.*, 2021, **14**, 2054–2066.
94 T. Tanaka, M. Takahashi, N. Nitta, A. Furukawa, A. Andoh, Y. Saito, Y. Fujiyama and K. Murata, *Digestion*, 2007, **74**, 199–205.
95 Y. Saito, T. Tanaka, A. Andoh, H. Minematsu, K. Hata, T. Tsujikawa, N. Nitta, K. Murata and Y. Fujiyama, *World J. Gastroenterol.*, 2007, **13**, 3977.
96 P. Gkolfakis, P. D. Siersema, G. Tziatzios, K. Triantafyllou and I. S. Papanikolaou, *Ann. Gastroenterol.*, 2020, **33**, 330.
97 E. Kailla, F. Rezai, A. K. Kansci, O. Akande and J. Gossage, *Surg. Endosc.*, 2023, **37**, 2476–2484.
98 S. Rejchrt, M. Kopáčová, J. Bártová, Z. Vacek and J. Bureš, *Folia Gastroenterol. Hepatol.*, 2009, **7**, 7–11.
99 O. N. Rincon, A. H. Madrigal, B. M. Rodriguez, C. G. Asanza, E. C. Arregui and P. M. Fernandez-Pacheco, *Endoscopy*, 2011, **43**, E189–E190.
100 Y. Yang, Y. Yang, Z. Hou, T. Wang, P. Wu, L. Shen, P. Li, K. Zhang, L. Yang and S. Sun, *Front. Bioeng. Biotechnol.*, 2023, **11**, 1327517.
101 Y. Wen, Y. Li, R. Yang, Y. Chen, Y. Shen, Y. Liu, X. Liu, B. Zhang and H. Li, *Mater. Today Bio*, 2024, **29**, 101259.
102 Z. Jin, K. Wu, J. Hou, K. Yu, Y. Shen and S. Guo, *Biomaterials*, 2018, **153**, 49–58.
103 H. L. Chen, W. Q. Shen and K. Liu, *Dis. Esophagus*, 2017, **30**, 1–16.

104 E. Jeon, J. M. Kang, G. H. Bae, C. H. Zeng, S. Shin, B. Lee, W. Park, J. H. Park and J. Lee, *Adv. Healthcare Mater.*, 2022, **11**, 2200389.
105 Y. Zhu, C. Hu, B. Li, H. Yang, Y. Cheng and W. Cui, *Acta Biomater.*, 2013, **9**, 8328–8336.
106 J. Y. Liu, Z. M. Wang, K. Q. Wu, J. Li, W. L. Chen, Y. Y. Shen and S. R. Guo, *Biomaterials*, 2015, **53**, 592–599.
107 R. C. Sabatelle, Y. L. Colson, U. Sachdeva and M. W. Grinstaff, *Mol. Pharmaceutics*, 2024, **21**, 3103–3120.
108 M. Shaikh, N. R. Choudhury, R. Knott and S. Garg, *Mol. Pharmaceutics*, 2015, **12**, 2305–2317.
109 K. Welén and J.-E. Damber, *Rev. Endocr. Metab. Disord.*, 2022, **23**, 1221–1231.
110 K. Stamatelou and D. S. Goldfarb, *Healthcare*, 2023, **11**, 424..
111 H. Dong, Y. Peng, L. Li and X. Gao, *Asian J. Urol.*, 2018, **5**, 94–100.
112 K.-W. Kim, Y. H. Choi, S. B. Lee, Y. Baba, H.-H. Kim and S.-H. Suh, *Comput. Math. Methods Med.*, 2017, **2017**, 5172641.
113 D. Lange, S. Bidnur, N. Hoag and B. H. Chew, *Nat. Rev. Urol.*, 2015, **12**, 17–25.
114 G. Bhagwat, W. O'Connor, I. Grainge and T. Palanisami, *Front. Microbiol.*, 2021, **12**, 687118.
115 P. Amado, S. K. Zheng, D. Lange, D. Carugo, S. L. Waters, D. Obrist, F. Burkhard and F. Clavica, *Front. Urol.*, 2024, **3**, 1335414.
116 A. De Grazia, G. LuTheryn, A. Meghdadi, A. Mosayyebi, E. J. Espinosa-Ortiz, R. Gerlach and D. Carugo, *Micromachines*, 2020, **11**, 408.
117 V. Bernasconi, M. Tozzi, A. Pietropaolo, V. De Coninck, B. K. Somani, T. Tailly, E. Bres-Niewada, I. Mykoniatis, A. Gregori and M. Talso, *Cent. Eur. J. Urol.*, 2023, **76**, 49.
118 N. Venkatesan, S. Shroff, K. Jayachandran and M. Doble, *J. Endourol.*, 2010, **24**, 191–198.
119 B. Domingues, M. Pacheco, J. E. de la Cruz, I. Carmagnola, R. Teixeira-Santos, M. Laurenti, F. Can, K. Bohinc, F. Moutinho and J. M. Silva, *Adv. Ther.*, 2022, **5**, 2100158.
120 Y. Wu, S. Liu, Y. Fan, J. Li, Y. Deng, P. Yu, C. Ning and J. Zhai, *Adv. Colloid Interface Sci.*, 2025, 103542.
121 E. O. Kehinde, V. O. Rotimi, A. Al-Hunayan, H. Abdul-Halim, F. Boland and K. A. Al-Awadi, *J. Endourol.*, 2004, **18**, 891–896.
122 Y. Barghouthy, O. Wiseman, E. Ventimiglia, J. Letendre, J. Cloutier, M. Daudon, F. Kleinclauss, S. Doizi, M. Corrales and O. Traxer, *World J. Urol.*, 2021, 1–7.
123 M. Tunney, P. Keane, D. Jones and S. Gorman, *Biomaterials*, 1996, **17**, 1541–1546.
124 Y. X. Wu, E. J. Choi, A. A. Vu, P. Jiang, S. N. Ali, R. M. Patel, J. Landman and R. V. Clayman, *ACS Omega*, 2023, **8**, 29003–29011.
125 O. Wiseman, E. Ventimiglia, S. Doizi, F. Kleinclauss, J. Letendre, J. Cloutier and O. Traxer, *J. Urol.*, 2020, **204**, 769–777.
126 M. Pacheco, J. M. Silva, I. M. Aroso, E. Lima, A. A. Barros and R. L. Reis, *Urinary Stents: Current State and Future Perspectives*, Springer International Publishing, Cham, 2022, pp. 197–208.
127 N. Tomer, E. Garden, A. Small and M. Palese, *J. Urol.*, 2021, **205**, 68–77.
128 Boston Scientific, TriaTM Ureteral Stent Unlike any other, https://www.bostonscientific.com/content/dam/bostonscientific/uro-wh/portfolio-group/StentVentures/tria/URO-554016-AC_Tria-eBrochure-Dec2022-Update.pdf, (accessed December 2022).
129 T. Yoshida, K. Takemoto, Y. Sakata, T. Matsuzaki, Y. Koito, S. Yamashita, I. Hara, H. Kinoshita and T. Matsuda, *Sci. Rep.*, 2021, **11**, 10337.
130 A. O. Kadlec, C. S. Ellimoottil, K. A. Greco and T. M. Turk, *J. Urol.*, 2013, **190**, 937–941.
131 K. Hendlin, E. Korman and M. Monga, *J. Endourol.*, 2012, **26**, 271–274.
132 K. Hu, Z. Hou, Y. Huang, X. Li, X. Li and L. Yang, *Front. Bioeng. Biotechnol.*, 2024, **12**, 1373130.
133 Y. Zhang, J. He, H. Chen and C. Xiong, *J. Biomater. Appl.*, 2021, **35**, 720–731.
134 A. A. Barros, C. Oliveira, A. J. Ribeiro, R. Autorino, R. L. Reis, A. R. C. Duarte and E. Lima, *World J. Urol.*, 2018, **36**, 277–283.
135 D. Tie, H. Liu, R. Guan, P. Holt-Torres, Y. Liu, Y. Wang and N. Hort, *Acta Biomater.*, 2020, **116**, 415–425.
136 S. A. Khan, Z. U. Rahman, Z. Cai, O. Jiang and G. Xu, *J. Drug Delivery Sci. Technol.*, 2024, **100**, 106039.
137 B. H. Chew, P. A. Cadieux, G. Reid and J. D. Denstedt, *J. Endourol.*, 2006, **20**, 949–958.
138 D. Margel, M. Mizrahi, G. Regev-Shoshani, M. Ko, M. Moshe, R. Ozalvo, L. Shavit-Grievink, J. Baniel, D. Kedar, O. Yossepowitch, D. Lifshitz, A. Nadu, D. Greenberg and Y. Av-Gay, *PLoS One*, 2017, **12**, e0174443.
139 K. H. Homeyer, M. J. Goudie, P. Singha and H. Handa, *ACS Biomater. Sci. Eng.*, 2019, **5**, 2021–2029.
140 Q. Yao, J. Zhang, G. Pan and B. Chen, *ACS Appl. Mater. Interfaces*, 2022, **14**, 36473–36486.
141 R. G. Elfarargy, M. Sedki, F. A. Samhan, R. Y. A. Hassan and I. M. El-Sherbiny, *J. Genet. Eng. Biotechnol.*, 2023, **21**, 92.
142 L. Gao, Y. Wang, Y. Li, M. Xu, G. Sun, T. Zou, F. Wang, S. Xu, J. Da and L. Wang, *Acta Biomater.*, 2020, **114**, 117–132.
143 M. Lenzuni, F. Fiorentini, M. Summa, R. Bertorelli, G. Suarato, G. Perotto and A. Athanassiou, *Int. J. Biol. Macromol.*, 2024, **257**, 128560.
144 A. E. Krambeck, R. S. Walsh, J. D. Denstedt, G. M. Preminger, J. Li, J. C. Evans and J. E. Lingeman, *J. Urol.*, 2010, **183**, 1037–1043.
145 J. Hu, Z. Wang, H. Hu, J. Zhao, H. Li, X. Zhang, J. Bi and J. Li, *Acta Biomater.*, 2023, **172**, 321–329.
146 L. R. Duan, L. Li, Z. Y. Zhao, X. Q. Wang, Z. Z. Zheng, F. Li and G. Li, *ACS Biomater. Sci. Eng.*, 2023, **10**, 607–619.
147 F. Soria, S. D. Aznar-Cervantes, J. E. de la Cruz, A. Budia, J. Aranda, J. P. Caballero, A. Serrano and F. M. S. Margallo, *Polymers*, 2022, **14**, 3059.
148 F. Soria, J. E. Delacruz, S. D. Aznar-Cervantes, J. Aranda, L. Martinez-Pla, M. Cepeda, A. Pérez-Lanzac, G. Bueno and F. M. Sánchez-Margallo, *Minerva Urol. Nephrol.*, 2023, **75**, 194–202.

149 T. C. Bellos, S. N. Katsimperis, S. G. Kapsalos-Dedes, L. I. Tzelves, N. A. Kostakopoulos, I. C. Mitsogiannis, I. M. Varkarakis, A. G. Papatsoris and C. N. Deliveliotis, *J. Clin. Pharmacol.*, 2023, **63**, 1091–1100.
150 Y.-C. Tham, X. Li, T. Y. Wong, H. A. Quigley, T. Aung and C.-Y. Cheng, *Ophthalmology*, 2014, **121**, 2081–2090.
151 R. N. Weinreb, T. Aung and F. A. Medeiros, *Jama*, 2014, **311**, 1901–1911.
152 P. A. Newman-Casey, A. L. Robin, T. Blachley, K. Farris, M. Heisler, K. Resnicow and P. P. Lee, *Ophthalmology*, 2015, **122**, 1308–1316.
153 H. Öhnell, A. Heijl, H. Anderson and B. Bengtsson, *Acta Ophthalmol.*, 2017, **95**, 281–287.
154 G. Gazzard, E. Konstantakopoulou, D. Garway-Heath, A. Garg, V. Vickerstaff, R. Hunter, G. Ambler, C. Bunce, R. Wormald and N. Nathwani, *Lancet*, 2019, **393**, 1505–1516.
155 A. Sheybani, R. Scott, T. W. Samuelson, M. Y. Kahook, D. I. Bettis, I. I. K. Ahmed, J. D. Stephens, D. Kent, T. J. Ferguson and L. W. Herndon, *Ophthalmol. Ther.*, 2020, **9**, 1–14.
156 J. Jabłońska, K. Lewczuk, J. Konopińska, Z. Mariak and M. Rękas, *Acta Ophthalmol.*, 2022, **100**, e327–e338.
157 T. S. Acott and M. J. Kelley, *Exp. Eye Res.*, 2008, **86**, 543–561.
158 M. Johnson, *Exp. Eye Res.*, 2006, **82**, 545–557.
159 R. David, L. Zangwill, D. Briscoe, M. Dagan, R. Yagev and Y. Yassur, *Br. J. Ophthalmol.*, 1992, **76**, 280–283.
160 M. M. Geloneck, E. L. Crowell, E. B. Wilson, B. E. Synder, A. Z. Chuang, L. A. Baker, N. P. Bell and R. M. Feldman, *J. Glaucoma*, 2015, **24**, 130–134.
161 Z. Zhang, X. Wang, J. B. Jonas, H. Wang, X. Zhang, X. Peng, R. Ritch, G. Tian, D. Yang, L. Li, J. Li and N. Wang, *Acta Ophthalmol.*, 2014, **92**, e475–e480.
162 B. C. H. Ang, S. Y. Lim and S. Dorairaj, *Eye*, 2020, **34**, 168–177.
163 S. D. Vold, L. Voskanyan, M. Tetz, G. Auffarth, I. Masood, L. Au, I. I. K. Ahmed and H. Saheb, *Ophthalmol. Ther.*, 2016, **5**, 161–172.
164 M. S. Malvankar-Mehta, Y. N. Chen, Y. Iordanous, W. W. Wang, J. Costella and C. M. Hutnik, *PLoS One*, 2015, **10**, e0128146.
165 W. S. Shalaby, J. Jia, L. J. Katz and D. Lee, *J. Cataract Refractive Surg.*, 2021, **47**, 385–399.
166 I. I. K. Ahmed, T. De Francesco, D. Rhee, C. McCabe, B. Flowers, G. Gazzard, T. W. Samuelson and K. Singh, *Ophthalmology*, 2022, **129**, 742–751.
167 I. I. K. Ahmed, A. Fea, L. Au, R. E. Ang, P. Harasymowycz, H. D. Jampel, T. W. Samuelson, D. F. Chang, D. J. Rhee and COMPARE Investigators, *Ophthalmology*, 2020, **127**, 52–61.
168 I. C. Pereira, R. van de Wijdeven, H. M. Wyss, H. J. Beckers and J. M. den Toonder, *Eye*, 2021, **35**, 3202–3221.
169 M. Balas and D. J. Mathew, *Vision*, 2023, **7**, 54.
170 M. Lenzhofer, I. Kersten-Gomez, A. Sheybani, H. Gulamhusein, C. Strohmaier, M. Hohensinn, H. Burkhard Dick, W. Hitzl, L. Eisenkopf and F. Sedarous, *Clin. Exp. Ophthalmol.*, 2019, **47**, 581–587.
171 X. Yang, Y. Zhao, Y. Zhong and X. Duan, *BMC Ophthalmol.*, 2022, **22**, 1–15.
172 F. A. Medeiros, T. R. Walters, M. Kolko, M. Coote, M. Bejanian, M. L. Goodkin, Q. Guo, J. Zhang, M. R. Robinson and R. N. Weinreb, *Ophthalmology*, 2020, **127**, 1627–1641.
173 S. S. Tan and T. T. Wong, *Asia-Pac. J. Ophthalmol.*, 2025, **14**, 100163.
174 I. Vagiakis, E. P. Papadopoulou, E. Amaxilati, G. N. Tsiropoulos, A. G. Konstas and G. D. Panos, *Drug Des., Dev. Ther.*, 2025, **19**, 703–714.
175 I. P. Singh, L. A. Voskanyan, K. M. Barber, J. H. Burden, L. Connolly, L. J. Katz, D. W. Usner, A. C. Kothe and T. Navratil, *Ther. Adv. Ophthalmol.*, 2025, **17**, 25158414241310275.
176 S. Teymoorian and J. Kaur, *Clin. Ophthalmol.*, 2025, **19**, 157–166.
177 X.-Z. Chen, Z.-Q. Liang, K.-Y. Yang, K. Lv, Y. Ma, M.-Y. Li and H.-J. Wu, *Front. Med.*, 2022, **9**, 804847.
178 G. Song, H. Q. Zhao, Q. Liu and Z. Fan, *Bioact. Mater.*, 2022, **17**, 488–495.
179 M. H. Emara, M. H. Ahmed, A. S. Mohammed, M. I. Radwan and A. M. Mahros, *Eur. J. Gastroenterol. Hepatol.*, 2021, **33**, 967–973.
180 R. Lam and T. Muniraj, *World J. Gastroenterol.*, 2021, **27**, 6357.
181 T. H. Lee, *Clin. Endosc.*, 2013, **46**, 260–266.
182 M. Battistel, M. Senzolo, A. Ferrarese, A. Lupi, U. Cillo, P. Boccagni, G. Zanus, R. Stramare, E. Quaia and P. Burra, *Cardiovasc. Interventional Radiol.*, 2020, **43**, 749–755.
183 Y. Tian, J. Zhang, J. Cheng, G. Wu, Y. Zhang, Z. Ni and G. Zhao, *J. Appl. Polym. Sci.*, 2021, **138**, 49656.
184 B. Meng, J. Wang, N. Zhu, Q.-Y. Meng, F.-Z. Cui and Y.-X. Xu, *J. Mater. Sci.: Mater. Med.*, 2006, **17**, 611–617.
185 Y. Zhao, J. Bai, F. Xue, R. Zeng, G. Wang, P. K. Chu and C. Chu, *Smart Mater. Manuf.*, 2023, **1**, 100022.
186 Y. Zhang, K. Chen, H. Liu, Y. Shao, C. Chu, F. Xue and J. Bai, *J. Mater. Sci.*, 2020, **55**, 17170–17182.
187 L. Guo, L. Yu, Q. Zhao, X. Gong, H. Xie, G. Yuan, B. Li and X. Wan, *Biomed. Mater.*, 2021, **16**, 025010.
188 Y. Chen, J. Yan, Z. Wang, S. Yu, X. Wang, Z. Yuan, X. Zhang, C. Zhao and Q. Zheng, *Mater. Sci. Eng., C*, 2014, **42**, 116–123.
189 Y. Chen, J. Yan, X. Wang, S. Yu, Z. Wang, X. Zhang, S. Zhang, Y. Zheng, C. Zhao and Q. Zheng, *Biometals*, 2014, **27**, 1217–1230.
190 Y. Liu, S. Zheng, N. Li, H. Guo, Y. Zheng and J. Peng, *Mater. Lett.*, 2016, **179**, 100–103.
191 H. Peng, K. Fan, R. Zan, Z.-J. Gong, W. Sun, Y. Sun, W. Wang, H. Jiang, J. Ni and T. Suo, *Acta Biomater.*, 2021, **128**, 514–522.
192 A. I. G. Q. Ltd, a Q3 Medical Devices Ltd Company, Receives European CE Mark Approval for UNITY-B Biodegradable Stent, https://www.prnewswire.com/news-releases/amg-international-gmbh-a-q3-medical-devices-ltd-company-receives-european-ce-mark-approval-for-unity-b-biodegradable-stent-301298110.html, (accessed 24 June 2021).

193 J. S. Sohn, J. I. Jin, M. Hess and B. W. Jo, *Polym. Chem.*, 2010, **1**, 778–791.
194 J. W. Lee, S.-G. Yang and K. Na, *Int. J. Pharm.*, 2012, **427**, 276–283.
195 K. T. Suk, J. W. Kim, H. S. Kim, S. K. Baik, S. J. Oh, S. J. Lee, H. G. Kim, D. H. Lee, Y. H. Won and D. K. Lee, *Gastrointest. Endosc.*, 2007, **66**, 798–803.
196 J. J. Y. Sung, *J. Ind. Microbiol.*, 1995, **15**, 152–155.
197 F. Yang, Z. Ren, Q. Chai, G. Cui, L. Jiang, H. Chen, Z. Feng, X. Chen, J. Ji, L. Zhou, W. Wang and S. Zheng, *Sci. Rep.*, 2016, **6**, 21714.
198 R. L. Siegel, N. S. Wagle, A. Cercek, R. A. Smith and A. Jemal, *Ca-Cancer J. Clin.*, 2023, **73**, 233–254.
199 A. Lueders, G. Ong, P. Davis, J. Weyerbacher and J. Saxe, *Am. J. Surg.*, 2022, **224**, 217–227.
200 L. E. Targownik, B. M. Spiegel, J. Sack, O. J. Hines, G. S. Dulai, I. M. Gralnek and J. J. Farrell, *Gastrointest. Endosc.*, 2004, **60**, 865–874.
201 Y. K. Cho, S. W. Kim, B. I. Lee, K. M. Lee, C. H. Lim, J. S. Kim, J. H. Chang, J. M. Park, I. S. Lee, M. G. Choi, K. Y. Choi and I. S. Chung, *Gut Liver*, 2011, **5**, 165–170.
202 L. Q. Yao, Y. S. Zhong, M. D. Xu, J. M. Xu, P. H. Zhou and X. L. Cai, *World J. Gastroenterol.*, 2011, **17**, 3342–3346.
203 T. Kuwai, T. Yamaguchi, H. Imagawa, S. Yoshida, H. Isayama, T. Matsuzawa, T. Yamada, S. Saito, M. Shimada, N. Hirata, T. Sasaki, K. Koizumi, I. Maetani and Y. Saida, *Dig. Endosc.*, 2019, **31**, 51–58.
204 J. S. Kim, W. S. Lee, C. Y. Chung, H. C. Park, D. S. Myung, C. Y. Oak, M. Y. Kim, M. O. Jang, S. J. Kang, H. C. Jang, S. B. Cho, H. S. Kim and Y. E. Joo, *Gastroenterol. Res. Pract.*, 2015, **2015**, 416142.
205 S. J. Kim, H. W. Kim, S. B. Park, D. H. Kang, C. W. Choi, B. J. Song, J. B. Hong, D. J. Kim, B. S. Park and G. M. Son, *Surg. Endosc.*, 2015, **29**, 3499–3506.
206 I. Balciscueta, Z. Balciscueta, N. Uribe and E. García-Granero, *Int. J. Colorectal Dis.*, 2020, **35**, 1439–1451.
207 J. E. van Hooft, J. V. Veld, D. Arnold, R. G. H. Beets-Tan, S. Everett, M. Götz, E. E. van Halsema, J. Hill, G. Manes, S. Meisner, E. Rodrigues-Pinto, C. Sabbagh, J. Vandervoort, P. J. Tanis, G. Vanbiervliet and A. Arezzo, *Endoscopy*, 2020, **52**, 389–407.
208 M. Mashar, R. Mashar and S. Hajibandeh, *Int. J. Colorectal Dis.*, 2019, **34**, 773–785.
209 Z. P. Yang, Q. Wu, F. Wang, X. F. Ye, X. S. Qi and D. M. Fan, *Int. J. Med. Sci.*, 2013, **10**, 825–835.
210 J. Ferreira-Silva, R. Medas, M. Girotra, M. Barakat, J. H. Tabibian and E. Rodrigues-Pinto, *Gastroenterol. Res. Pract.*, 2022, **2022**, 6774925.
211 S. Rejchrt, M. Kopacova, J. Brozik and J. Bures, *Endoscopy*, 2011, **43**, 911–917.
212 M. Braendengen, K. M. Tveit, A. Berglund, E. Birkemeyer, G. Frykholm, L. Pahlman, J. N. Wiig, P. Byström, K. Bujko and B. Glimelius, *J. Clin. Oncol.*, 2008, **26**, 3687–3694.
213 E. B. Ludmir, M. Palta, C. G. Willett and B. G. Czito, *Cancer*, 2017, **123**, 1497–1506.
214 M. Arafat, P. Fouladian, A. Blencowe, H. Albrecht, Y. Song and S. Garg, *J. Controlled Release*, 2019, **308**, 209–231.
215 S. I. Jang, K. T. Lee, J. S. Choi, S. Jeong, D. H. Lee, Y. T. Kim, S. H. Lee, J. S. Yu and D. K. Lee, *Endoscopy*, 2019, **51**, 843–851.
216 S. I. Jang, S. J. Lee, S. Jeong, D. H. Lee, M. H. Kim, H. J. Yoon and D. K. Lee, *Gut Liver*, 2017, **11**, 567–573.
217 H. D. Zhu, J. H. Guo, M. Huang, J. S. Ji, H. Xu, J. Lu, H. L. Li, W. H. Wang, Y. L. Li, C. F. Ni, H. B. Shi, E. H. Xiao, W. F. Lv, J. H. Sun, K. Xu, G. H. Han, L. A. Du, W. X. Ren, M. Q. Li, A. W. Mao, H. Xiang, K. X. Zhang, J. Min, G. Y. Zhu, C. Su, L. Chen and G. J. Teng, *J. Hepatol.*, 2018, **68**, 970–977.